SEMMELWEIS EGYETEM

DOKTORI ISKOLA

Ph.D. értekezések

3113.

JAKAB ANNA

Onkológia
című program

Programvezető: Dr. Bödör Csaba, egyetemi tanár

Témavezetők: Dr. Micsik Tamás Szabolcs, egyetemi adjunktus

Microenvironment, systemic inflammatory response and tumor markers considering consensus molecular subtypes of colorectal cancer

Thesis

Anna Jakab, MD

Doctoral School of Semmelweis University

Division of Pathology and Oncology

Supervisor: Tamás Micsik, MD, Ph.D.

Official reviewer: Judit Halász, MD, Ph.D.

Tamás Szamosi, MD, Ph.D.

Head of the Complex Examination Committee:

Professor Kulka Janina, MD, D.Sc.

Members of the Complex Examination Committee:

Erika Tóth, MD, Ph.D.

Professor Béla Molnár, MD, D.Sc.

Budapest

2024

Table of Contents

List of Abbreviations

AI – Artificial Intelligence

AJCC – American Joint Committee on Cancer

ALC – Absolute Lymphocyte Count

ANC – Absolute Neutrophil Count

APC – Absolute Platelet Count

CA 19-9 – Carboanhydrate Antigen 19-9

CEA - Carcinoembryonic Antigen

CI – Confidence Interval

CK – Cytokeratin

CMS – Consensus Molecular Subtypes

CNN – Convolutional Neuronal Network

CRC – Colorectal Cancer

CRP – C Reactive Protein

dMMR – Mismatch Repair Deficient

EMT – Epithelio-Mesenchymal Transition

FFPE – Formalin Fixed Paraffin Embedded

FN – False Negative

FP – False Positive

GMS – Glasgow Microenvironment Score

HE – Hematoxylin-Eosin

HR – Hazard Ratio

IF – Invasive Front

IHC – Immunohistochemistry

KM – Klintrup-Makinen

mGPS – modified Glasgow Prognostic Score

M – Distant metastasis

ML – Machine Learning

MMR – Mismatch Repair

OS – Overall Survival

pMMR – Mismatch Repair proficient

pN – Pathological node stage

pT – Pathological tumor stage

SIR – Systemic Inflammatory Response

STM – Stroma – Tumor Marker score

TMA – Tissue Microarray

TME – Tumor microenvironment

TNM – Tumor, Node, Metastasis

TN – True Negative

TP – True Positive

TSR – Tumor-Stroma Ratio

$TSR_{software}$ – Software-Assisted TSR

TSR_{visual} – Visual TSR

UICC – Union for International Cancer Control

1. Introduction

1.1.The role of tumor microenvironment in colorectal cancer

One of the most prevalent malignant diseases is colorectal cancer (CRC), which is the second most frequent cause of cancer related deaths worldwide. As of now, the gold standard in staging CRC is the American Joint Committee on Cancer (AJCC), tumor, lymph node and metastasis (TNM) staging system, which is fundamental in the process of risk stratification and clinical decision making (1, 2). Besides the TNM system, multiple other prognosticators or predictive markers are available on a spectrum from the simplest histopathological, hematoxilin-eosin (HE) based feature to particular molecular subtypes or certain mutations (3, 4). Still, despite all the improvement in both diagnostic and therapeutic modalities, targeted agents are not suitable for all CRC patients, and while many of them could benefit from it, some present resistance (5).

Another aspect of cancer biology is the tumor microenvironment (TME), which is integral to malignant tumors, and provides comprehensive understanding of tumor aggressiveness and even of resistance to therapy, which makes TME derived markers ideal candidates as prognostic or predictive tools (6-8). Some features of TME in CRC could provide clinically relevant information, while also being readily available and simple, HE-based histopathological variables.

The Klintrup-Makinen (KM) (Figure 1) score describes the morphology of the intra- and peritumoral inflammatory infiltrate on HE-slides, with pronounced host-reaction resulting in overall better surival (9). The tumor-stroma ratio (TSR) characterizes the desmoplastic stromal reaction at the invasive front of the tumor(10, 11). Stroma-high (or TSR–high) tumors (Figure 1) are linked to a more agressive phenotype with notably poor prognosis and potential resistance to standard chemotherapy (12, 13). The combination of these two markers resulted in the Glasgow Microenvironment Score (GMS)(14), which further classifies CRC patients into low, intermediate or high risk groups (15).

1.2.Consensus molecular subtypes

In 2015, the consensus molecular subtyping consortium identified four subclasses of CRC – the so-called consensus molecular subtypes (CMS) – using transcriptome-based, gene expression pattern analysis (Figure 2) (4). These four classes represent distinct groups of CRC regarding their molecular status, biological behaviour, response to therapy, and to

some extent, histological appearance. Two of the CMSs, CMS1 and CMS4 are greatly determined by their microenvironment (16).

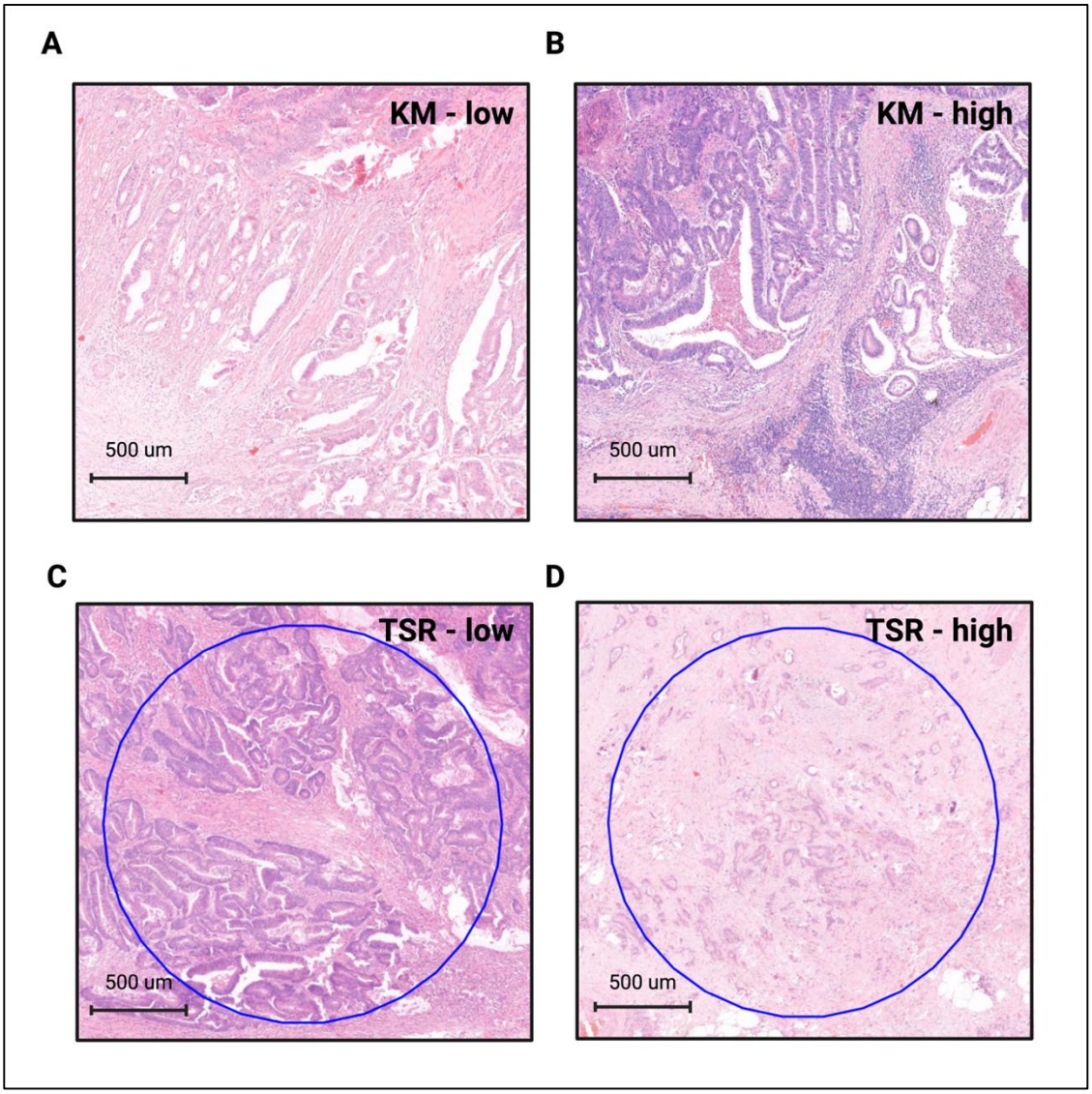

Figure 1: The Klintrup-Makinen (KM) grade and tumor-stroma ratio (TSR). In case of patchy, mild inflammation at the invasive front, cases are classified as KM-low (A). If there is a band- or cup-like, florid inflammatory infiltrate with destruction of tumor cells, cases are graded as KM-high (B). If stromal content is less than 50% of the examined area, cases are graded as TSR-low (C). If stromal content equals or exceeds 50% of this area, cases are graded as TSR-high (D). List of abbreviations: KM – Klintrup-Makinen grade, TSR – tumor-stroma ratio.

The CMS1, which is also known as „immune" subtype, exhibits abundant antitumoral inflammatory infiltrate and overexpression of genes associated with CD8+, T helper1 cell activation and T cell attracting chemokines (16), which might be explained by the abundance of mismatch repair deficiency (dMMR) and hypermutation in these tumors.

Meanwhile, the CMS4 or mesenchymal subtype displays pronounced stromal infiltration and TGFβ signaling (4, 17). Although currently available in the research field only, CMS classification seems promising, and might eventually play an important role in both predicting response to traditional agents and personalized therapy as well, since the usual targeted agents may be particularly ineffective in CMS4 tumors (18, 19).

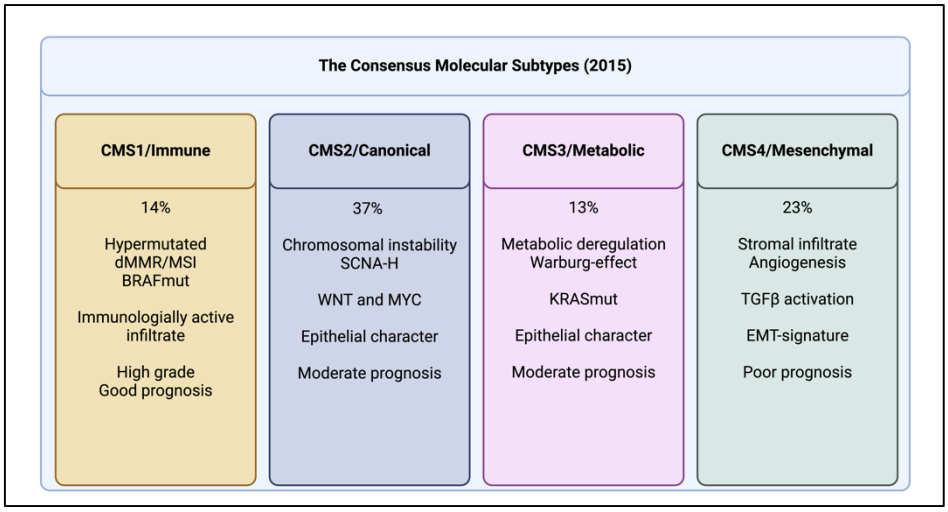

Figure 2: The consensus molecular subtypes (CMS) of colorectal cancer as described by Guinney et al (4).

1.1.The role of systemic host response in CRC

The host response observed microscopically in malignancies often presents as pronounced systemic inflammation concurrently, and the latter is often associated with poor outcome. A marked systemic inflammatory reaction (SIR) reflected by elevation of its markers, like C reactive protein (CRP), absolute neutrophil count (ANC) or lymphocyte count (ALC), or platelet count (APC), is often associated with poor prognosis in many cancer types, including CRC (20, 21). Some SIR markers might be associated with the TME, however, their link to CMS, or more precisely, CMS4, is unknown yet (22). Some components of the SIR can be examined in combination using composite ratios or cumulative scores. The modified Glasgow Prognostic Score (mGPS), consisting of serum albumin and CRP, is an endorsed indicator of systemic inflammatory processes in malignancies (23, 24). In CRC patients the mGPS accurately predicts outcomes, with a high mGPS score forecasting poor overall survival (OS) (23).

1.2.The role of tumor markers in CRC prognostics

Besides the aforementioned markers, routinely used tumor markers may also conveniently reflect tumor phenotype and predict patient outcome. Carcinoembryonic

antigen (CEA) and carbohydrate antigen 19-9 (CA19-9) are commonly used tumor markers in CRC follow-up, and while these might not have the same efficacy in monitoring recurrence (25), they might be practical in certain subgroups of CRC patients (26, 27). Although CEA and CA19-9 are not suited for screening purposes, their elevated levels are associated with advanced stages of CRC and therefore worse outcomes, and might be related to therapy resistance (28-30).

1.3.Challenges in TSR assessment

Even though TSR has great prognostic power, its assessment might pose some challenges. For example, one of such issues is the exclusion of multiple tissue types (e.g. lumina, mucus, necrosis, smooth muscle, large vessels, etc.), which is necessary when counting TSR, while making precise quantification and reproducibility problematic (10).

Deep learning-based digital image analysis systems in the medical field are a recent advance of the artifical intelligence (AI) and convolutional neural network (CNN) era. These innovations may aid the pathology workflow by accurate and precise identification and quantification of histological components, and had already shown robust performance in pattern recognition. A plausible application of this area is aiding the pathology workflow by accurate and reliable solutions for recognition and precise quantification of histological components. Some of these algorithms have presented robust performance in pattern recognition and outcome prediction, such as TSR or TME assessment (31-34), and in predicting certain molecular subtypes as well (35, 36). As per visual assessment, the accuray of these systems surpassed human professionals (33, 37), while analysis of whole slide images or multiple regions of interests could be executed effortlessly (38, 39). Nevertheless, many of these softwares are not available for the average healthcare worker as they were results of individual development, and some even require advanced programming skills (32, 38).

Altogether, these issues suggest the necessity of a widely accessible, convenient platform with the prospect of being incorporated into the routine histopathological procedures.

2. Objectives

2.1. Evaluating stromal component – machine learning (ML) as a potential tool

A key element of the dissertation was TSR evaluation and the difficulties associated with it. The objective of the authors was to consider a method that aids the precise quantification of TSR with the help of a commercially available, ML-based digital image analysis software. A crucial point was testing the accuracy of the software-aided TSR assessment and investigating the agreement with visual TSR evaluation. Of further focus was to compare the two methods in matters of prognostic power and relationship to clinicopathological variables.

2.2. The relationship between microenvironment, systemic markers and CMS

Our research was focused on TME markers, and systemic inflammation, due to their good reproducibility and availability in routine histopathological and clinical evaluation and also the CMS. The aim of the authors was to analyze the relationship between the aforementioned factors, as well as exploring and comparing their prognostic significance while assessing their influence on the biological behaviour of CRC.

To the authors' best knowledge, this is the first study that thoroughly evaluates the link between CMS, TME, SIR and tumor markers.

2.3. Assessing and developing a novel, TME and tumor marker based combined prognostic marker

Scoring systems comprising of semi-quantitative aspects of certain TME or systemic inflammation-based markers are no novelty in oncology. A combination of strong prognostic factors have the ability to further identify a subset of patients with particularly poor outcome. The authors' goal was to incorporate a key TME element and a clinically relevant systemic marker into a combined score similar to mGPS, and to examine its prognostic relevance.

3. Methods

3.1.Patients and slides

Altogether, 185 stage I-IV CRC patients were selected in a retrospective cohort. All patients underwent surgical resection and were diagnosed in the Institue of Pathology and Experimental Cancer Research (Budapest, Semmelweis University, Hungary) between 2009 and 2017. All relevant slides and formaline fixed paraffin embedded (FFPE) blocks were retrieved from the archives of the Institute. Slides containing the deepest site of invasion were scanned using Pannoramic 1000 scanner (3DHistech, Budapest, Hungary) equipped with a 40x objective.

Exclusion criteria included neoadjuvant treatment, death within 30 days of surgery, diagnosis of other malignancy in medical history. Anamnestic data and laboratory results were obtained via the internal medical database of Semmelweis University (MedSolution, T-Systems, Budapest, Hungary). Preoperative serum CA19-9 and CEA levels were measured routinely using Abbott Architect CA 19-9 XR immunoassay (Chicago, IL, United States of America) and Abbott Architect CEA immunoassay (Chicago, IL, United States of America). Staging and evaluating surgically resected CRC specimen was performed according to the UICC TNM classification, 8th edition.

The studies were approved by the Hungarian Scientific Council National Ethics Committee for Scientific Research (no. 216/2020).

3.2.Visual TME assessment

For TSR assessment, the area of interest was selected at the invasive front using a 10x objective. This “hotspot” area had to contain the highest percentage of stromal compartment. Furthermore, tumor cells had to be present at all four poles of the examined area.The stromal content was estimated per 5% increments. Tissue compartments consisting of necrotic debris, mucus, smooth muscle, nerves, and large vessels were excluded from the stromal compartment as recommended (10). In case the TSR was ≥50%, the case was classified as TSR-high, otherwise, it was classified as TSR-low (Figure 1).

The KM grade evaluates the inflammatory reaction in a semi-qunatitative manner. When there was no or insignificant increase in inflammatory cells at the invasive front, host reaction was graded as KM-low. In case of abundant, band- or cup-like infiltrate at the

margin with destructed tumor cells, the inflammation was classified as KM-high (Figure 1) (9).

The combination of KM grade and TSR gives a slightly more sophisticated notion on the local host response. The presence of extensive inflammation (KM-high) always results in GMS0 score, even with pronounced stromal infiltration, though, such cases are uncommon. When there isn't any prevalent inflammation (KM-low) nor stromal infiltration (TSR-low), the case is graded as GMS1. Abundant stromal content (TSR-high) in combination with weak inflammatory reaction yields a GMS2 score (14, 15).

All of the aforementioned parameters were graded by two independent observers (AJ and TM) in a blinded manner. The final results in cases of discordant scoring were determined after discussion between the two raters.

3.3.TME assessment using ML-based digital pathology software

The "hotspot" area selected for visual TSR assessment was evaluated using the ML-assisted software as well, which was annotated as a circular area of 3.77 mm^2 representing a 10x objective (Figure 3a).

To establish "gold standards" for validation of software performance, 52 cases were randomly selected. Different tissue types (tumor epithelia, smooth muscle, necrosis, background/lumina, stroma) were manually annotated within the hotspot area, which resulted in accurate quantification of each tissue compartment (Figure 3b.). These "gold standard" annotations were the basis of comparing the pathologist's and the software's performance.

The software of choice was the PatternQuant module of QuantCenter, which is the extension of SlideViewer (3DHistech, Budapest, Hungary). PatternQuant is a trainable, machine learning-based pattern recognition algorithm, which identifies certain tissue types based on texture patterns and hue intensity via wavelet transformation. An individually trained algorithm – so-called "scenario" –was created for all 185 slides, that could differentiate between five distinct patterns representing particular tissue compartments, also known as "clusters"(Figure 4). Each scenario is made up of five (or less) clusters, which were in most cases tumor epithelium, stroma, smooth muscle, necrosis/debris, and background (Figure 4).

All cases were assessed by both software ($TSR_{software}$) and visual analysis (TSR_{visual}).

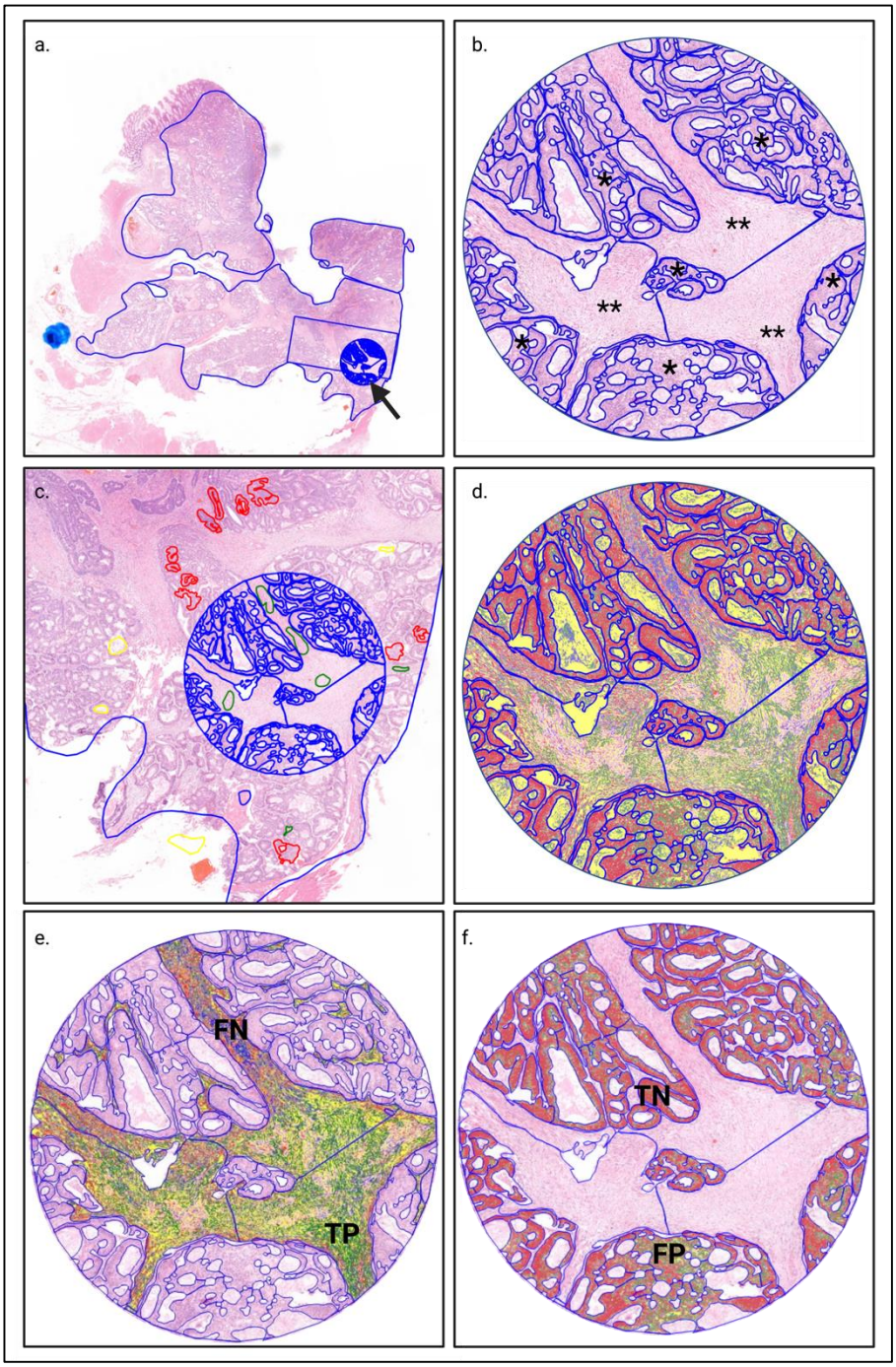

Figure 3: Manual annotations of the gold standard slides and training of scenarios. a: arrow denotes hotspot area (size: 3.77 mm2) at the invasive front (IF). b: Tissue compartments, like tumor epithelium, stroma, etc were manually annotated to serve as gold standard for validation. (marks tumor epithelium** marks the stromal compartment.) Each scenario was trained by outlining certain tissue types (clusters, small foci marked in red, yellow, green) (c), and then it was applied on the selected hotspot areas (d). With the help of the gold standard annotations, the accuracy, sensitivity and specificity were accurately calculated for ML-based quantification. For example, in the case of stromal compartment recognition, if areas were correctly labeled as stroma by the software within the*

gold standard stromal region, these were classified as true positive (TP), while stromal areas labeled incorrectly as necrosis, tumor, etc. were classified as false negative (FN) (Figure 3.e.). If there were any areas labeled as stroma within the tumor or any other compartment, these were classified as false positive (FP), and areas labeled as non-stromal parts in the corresponding compartment were classified as true negative (TN)(Figure 3.f.). Vice versa, when determining accuracy of tumor recognition, all areas labeled as tumor within the tumor compartment were classified as TP, and all tumorous areas marked as non-tumor (stroma, necrosis, etc.) in the same area were rated as FN, and so on.

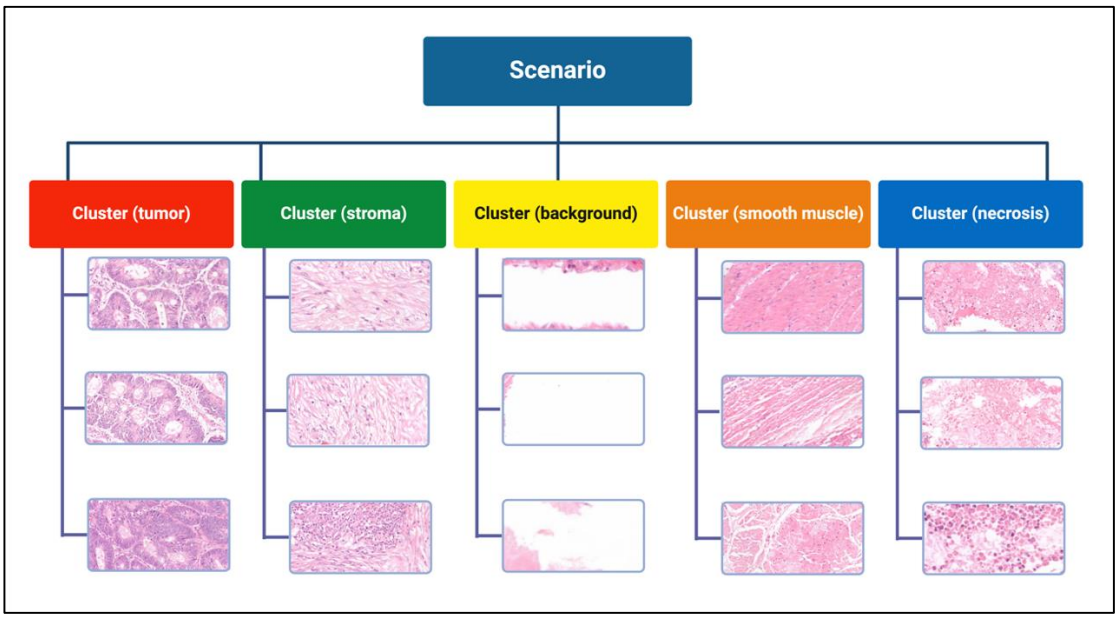

Figure 4: Each scenario was individually trained based on annotations of certain tissue types (clusters) made by the observers. Tumor epithelium, stromal compartment, background (lumina), smooth muscle and necrosis were then identified and recognized by the software based on the trained scenarios. At most ten representative annotations per cluster, and a maxmum of five clusters were allowed per scenario.

3.4.Microarray construction and immunohistochemistry (IHC)

Tissue microarray (TMA) blocks containing 6x9 cores (core diameter: 2mm) selected from surgically derived FFPE blocks of 167 patients were created using TMA Master1000 (3DHistech, Budapest, Hungary). At least two representative cores were selected per case from the tumor centre. Non-neoplastic kidney samples were used as stain and orientation controls in each block. IHC was performed on 4 um thick sections of the TMAs. For mismatch repair status (MMR) assessment, anti-MLH1, anti-PMS2, anti-MSH2, and anti-MSH6 primary stains were used and evaluated as recommended (40). Further CMS subtyping was carried out on proficient MMR (pMMR) samples using anti-

pancytokeratin (CK), anti-CDX2, anti-FRMD6, and anti-ZEB1 stains as described by Ten Hoorn et al (41). For further details of IHC, please see Table 2.

Table 1: Parameters of tumor characteristics and blood samples evaluated in the study. Abbreviations: TME – tissue microenvironment, TSR – tumor-stroma ratio, KM grade – Klintrup-Makinen grade, GMS – Glasgow microenvironment score, CMS – consensus molecular subtype, dMMR – mismatch repair deficient, SIR – systemic inflammatory repsonse, mGPS – modified Glasgow prognostic score, CRP – C reactive protein, ANC – absolute neutrophil count, ALC – absolute lymphocyte count, CEA – carcioembryonic antigen, CA 19-9 – cancer antigen 19-9, STM – stroma-tumor marker score.

Marker type			Cutoff used for marker
TME	TSR_{visual} and $TSR_{software}$, n=185	TSR-low TSR-high	less than 50% stromal content of hotspot
	KM, n=185	KM-low KM-high	According to Klintrup et al. (9)
	GMS, n=185	GMS 0 GMS 1 GMS 2	KM high KM low and TSR low KM low and TSR high
Consensus molecular subtypes, n=155		CMS1: dMMR CMS2/3: Epithelial CMS4: Mesenchymal	According to Trinh et al. (42)
SIR	mGPS, n=95	mGPS 0 mGPS 1 mGPS 2	CRP-low, albumin-low CRP-high, albumin-high albumin-low and CRP-high
	Albumin, n=107	albumin-low albumin-high	<35 g/l
	CRP, n=149	CRP-low CRP-high	<10 mg/l
	ANC, n=170	ANC-low ANC-high	<4.85 G/l
	ALC, n=170	ALC-low ALC-high	<1.65 G/l
	APC, n=180	APC-low APC-high	<400 G/l
Tumor markers	CEA, n=155	CEA low CEA high	<5 ng/ml
	CA19-9, n=135	CA19-9 low CA19-9 high	<37 U/ml
Stroma-tumor marker score, n=135		STM0 STM1 STM2	TSR-low and CA19-9 low TSR-low and CA19-9 high or TSR-high and CA19-9 low TSR-high and CA19-9 high

*Table 2: Immunohistochemical reactions: List of primary antibodies and detection systems used during the immunohistochemical staining protocol. Primary antibodies denoted by * were incubated for 30 minutes, post primary antibodies and polymer were applied for 15 minutes each with the BOND Polymer Refine Detection Kit, DS9800 (Leica, Weitzlar, Germany). Primary antibodies denoted by ** were incubated for 90 minutes, post primary antibodies and polymer (Novolink Polymer DS, RE7150-CE (Leica, Weitzlar, Germany)) were incubated for 30 minutes each. All IHC reactions were counterstained with hematoxilin(incubation time: 4 minutes).*

Function	Primary antibody (clone ID)	Manufacturer	Dilution	Detection system (post primary and polymer)	Incubation and DAB (minutes, vendor)
Mismatch repair system (MMR)	MLH1* (G168-728)	CellMarque, Rocklin, CA, USA	1:100	BOND Polymer Refine Detection Kit, DS9800 (Leica, Weitzlar, Germany)	10, Polymer Refine Detection Kit, DS9800 (Leica, Weitzlar, Germany)
	MSH2* (DB15.82)	Diagnostic Biosystems, Pleasanton, CA, USA	1:100		
	MSH6 * (EP49)	Eptomics, Burlingame, CA, USA	1:75		
	PMS2* (EP51)		1:50		
Epithelial marker	CK* (AE1/AE3)	Dako, Carpinteria, CA, USA	1:150		
Instestinal marker	CDX2* (Dako-CDX2)		1:50		
Hippo pathway activation	FRMD6** (PA5-9865)	Thermo Fisher Scientific, Waltham, MA, USA	1:250	Novolink Polymer DS, RE7150-CE (Leica, Weitzlar, Germany)	2-10, Dako, Carpinteria, CA, USA
Epithelio-mesenchymal transition	ZEB1** (HPA027524)	Merck, Darmstadt, Germany	1:500		
Serotonin receptor	HTR2B** (HPA012867)		1:250		

Cytoplasmic staining of CK and FRMD6, nuclear staining of CDX2, as well as membranous and cytoplasmic staining of HTR2B were graded as low, moderate or high. In case of ZEB1, the presence of nuclear staining was scored as either present or absent. All CMS stains were graded in accordance with Ten Hoorn et al's recommendations (42).

Cases were classified as either epithelial (CMS2 and CMS3, collectively), or mesenchymal (CMS4).

All IHC reactions were assessed by two observers (AJ and TM).

3.5.CMS classification

Cases with dMMR were classified as CMS1. For pMMR tumors, CMS classification was performed using an online, TMA-based and validated, robust and reliable random forest classifier (https://crcclassifier.shinyapps.io/appTesting/), altough, this method doesn't differentiate between CMS2 and CMS3(41, 42). Briefly, four immunostains (ZEB1, HTRB2, FRMD6 and CDX2) were selected based on distinct gene expression profile differences in epithelial (all CMS2 and CMS3 cases, collectively) and mesenchymal (CMS4 tumors). In pMMR tumors, the stain intensity and content of these four stains in tumor epithelium correlates with their CMSs (41). Typically, low FRMD6 and HTR2B staining intensities, lack of nuclear ZEB1 expression and strong CDX2 stain correlates with epithelial subtypes (CMS2/3); while strong positive FRMD6 and HTR2B, loss of CDX2 and positive nuclear ZEB1 reaction is expected in mesenchymal CRCs (CMS4) (Figure 3) (42). In case the probability of a CMS was estimated higher than 0.6, the case was automatically labeled in concordance with the software. If the probability of estimated CMS was between 0.5 and. 0.6, the case was automatically excluded from our analysis. In total, 12 cases were excluded due to uncertain subtyping.

3.6.Creating a novel scoring system: the stroma – tumor marker score

To reflect the biological behaviour of certain cancer subtypes classified by TME and systemic response, a novel scoring system was established by combining CA19-9 and TSR, the most robust prognosticators independent of stage, into stroma-tumor marker (STM) score. In case of TSR-low and CA 19-9 low cases, STM 0 score was given. If either CA19-9 or TSR was classified as high, but the other marker as low, an STM 1 score was given. When both markers were classified as „high", STM 2 score was given (see Table 1).

3.7.Statistical analysis

Shapiro-Wilks test of normality was performed on the continuous variables. In order to determine the relationship between clinicopathological features and categorical variables, Chi-squared test was performed. Mann-Whitney U-test or Kruskal-Wallis H-test was performed to examine the correlation between clinicopathological features and

continuous variables. Cohen's Kappa (κ) was calculated to assess interobserver agreement between the visual and software classification of TSR.

The accuracy of stromal or tumoral compartment recognition of the ML-based software was calculated according to the following formula:

$$Accuracy = \frac{TP + TN}{TP + TN + FP + FN}$$

where TP = True Positive; TN = True Negative; FP = False Positive; FN = False Negative, which were calculated based on the gold standard annotations.

To demonstrate differences in overall survival (OS) we performed Kaplan-Meier survival analyses and log-rank statistics. OS was defined as the time between the date of surgery and the date of death from any cause. When no event was detected during the follow-up period, the date of the last follow-up was used for survival analyses.

Lastly, to determine, whether the investigated parameters were independent prognosticators of OS, uni- and multivariate Cox regression survival analyses were performed. All variables that reached $p<0.1$ in the univariate analysis were included for the multivariate analysis.

P values <0.05 were considered as statistically significant.

In this article, all statistical analyses were performed using IBM SPSS v26.0 (Armonk, New York, United States).

4. Results

4.1. Patient charactreristics

Out of the 185 patients who were included in our cohort, 155 patients had available CEA, and 135 patients had available CA19-9 results. CMS classification was carried out in 155 patients. Detailed demographic data is available in Table 3 and 4.

4.2.Software performance and interobserver agreement

Accuracy, sensitivity and specificity for tumor and stroma recognition can be seen in Table 5. Cohen's κ for TSR_{visual} between observers was 0.778, and between $TSR_{GoldStandard}$ and TSR_{visual} it was 0.711. κ values for between $TSR_{software}$ and TSR_{visual} were 0.472 ($p<0.001$ in all cases).

Table 5: The performance of the machine learning-based algorithm regarding stroma- and tumor recognition

	Sensitivity	Specificity	Accuracy
Tumor epithelium	67.1%	86.5%	80%
Stroma	64.6%	78.3%	72.4%

4.3.TME, SIR, tumor marker and CMS characteristics

Patients with TSR-high tumors were significantly associated with higher pT (p=0.043), pN (p<0.001) and M (p<0.001) (Table 3). Also, lymphatic and perineural invasion was significantly higher amongst TSR-high patients (p<0.001 and p=0.002). TSR correlated with age, CEA-high and CA19-9-high (p=0.022, p=0.029, p=0.035). Similarly, KM-low correlated with advanced pT, pN, stage and M-status (p=0.029, p=0.024, p=0.017 and p=0.009) and also, a tendency towards lymphatic invasion (p=0.093) was found (Table 3). As expected based on TSR and KM grading results, GMS was also associated similarly with clinicopathological features (Table 4). KM, TSR or GMS were not associated with any SIR markers (Table 6).

Elevation of serum CRP was associated with increasing stage (p=0.002), pT (p<0.001), distant metastasis (p=0.007), higher grade (p=0.027), vascular invasion (p=0.026), lymphatic invasion (p=0.032) and there was a trend towards perineural invasion (p=0.063) (Table 6). There was a significant correlation between ANC and higher pT (p=0.011) and a trend towards advanced pN (p=0.058) (Table 6). ALC did not correlate with any of the examined features, but with younger age (p=0.007).

Table 3: The relationship between tumor-stroma ratio (TSR), Klintrup-Makinen (KM) grade and clinicopathological features. The relationship between TME markers and clinicopathological features was assessed using Chi-squared test. Significant correlations were marked with bold font, while tendencies where p<0.1 were marked with italic font. In some cases, percentages do not add up to 100% precisely due to rounding. Abbreviations: TSR – tumor-stroma ratio, KM – Klintrup-Makinen, mGPS – modified Glasgow Prognostic Score, CMS – consensus molecular subtypes, CEA – carcinoembryonic antigen, CA 19-9 – Carbohydrate antigen 19-9

Clinico-pathological features	All patients (n=185*)	TSR (n=185)			KM grade (n=185)		
		TSR-low (n=121)	TSR-high (n=64)	p value	KM-low (n=123)	KM-high (n=62)	p value
Age (n=185)				**p=0.022**			p=0.237
<65	65 (35%)	**34 (28%)**	**31 (48%)**		45 (37%)	20 (32%)	
65-74	77 (42%)	**56 (46%)**	**21 (33%)**		54 (44%)	23 (37%)	
75<	43 (23%)	**31 (26%)**	**12 (19%)**		24 (20%)	19 (31%)	
Sex (n=185)				p=0.353			p=0.434
Female	97 (52%)	60 (50%)	37 (58%)		67 (55%)	30 (48%)	
Male	88 (48%)	61 (50%)	27 (42%)		56 (46%)	32 (52%)	
Location (n=185)				p=0.350			p=0.488
Right colon	75 (41%)	53 (44%)	22 (34%)		47 (38%)	28 (45%)	
Left colon	58 (31%)	34 (28%)	24 (37.5%)		42 (34%)	16 (26%)	
Rectum	52 (28%)	34 (28%)	18 (28%)		35 (28%)	18 (29%)	
pT (n=185)				**p=0.043**			**p=0.029**
pT1	2 (1%)	**2 (2%)**	**0 (0%)**		**0 (0%)**	**2 (3%)**	
pT2	34 (18%)	**28 (23%)**	**6 (9%)**		**22 (18%)**	**12 (19%)**	
pT3	134 (72%)	**84 (69%)**	**50 (78%)**		**87 (71%)**	**47 (76%)**	
pT4	15 (8%)	**7 (6%)**	**8 (13%)**		**14 (11%)**	**1 (2%)**	
pN (n=184)				**p<0.001**			**p=0.024**
pN0	82 (45%)	**66 (55%)**	**16 (25%)**		**47 (39%)**	**35 (57%)**	
pN1	67 (36%)	**37 (31%)**	**30 (47%)**		**46 (38%)**	**21 (34%)**	
pN2	35 (19%)	**17 (14%)**	**18 (28%)**		**29 (24%)**	**6 (10%)**	
M (n=185)				**p<0.001**			**p=0.009**
M0	143 (77%)	**104 (86%)**	**39 (61%)**		**88 (72%)**	**55 (89%)**	
M1	42 (23%)	**17 (14%)**	**25 (39%)**		**35 (29%)**	**7 (11%)**	
Stage (n=185)				**p<0.001**			**p=0.017**
I	26 (14%)	**23 (19%)**	**3 (5%)**		**16 (13%)**	**10 (16%)**	
II	48 (26%)	**37 (31%)**	**11 (17%)**		**25 (20%)**	**23 (37%)**	
III	69 (37%)	**44 (36%)**	**25 (39%)**		**47 (38%)**	**22 (36%)**	
IV	42 (23%)	**17 (14%)**	**25 (39%)**		**35 (29%)**	**7 (11%)**	
Grade (n=185)				p=0.108			p=0.629
Low/moderate	161 (87%)	109 (90%)	52 (81%)		106 (86%)	55 (89%)	
High	24 (13%)	12 (10%)	12 (19%)		17 (14%)	7 (11%)	
Lymphatic invasion (n=185)				**p<0.001**			*p=0.093*
Not present	122 (66%)	**94 (78%)**	**28 (44%)**		*76 (62%)*	*46 (74%)*	
Present	63 (34%)	**27 (22%)**	**36 (56%)**		*47 (38%)*	*16 (26%)*	
Perineural invasion (n=185)				**p=0.002**			p=0.247
Not present	170 (92%)	**117 (97%)**	**53 (83%)**		111 (90%)	59 (95%)	
Present	15 (8%)	**4 (3%)**	**11 (17%)**		12 (10%)	3 (5%)	
Vascular invasion (n=185)				p=0.099			p=0.130
Not present	143 (77%)	98 (81%)	45 (70%)		91 (74%)	52 (84%)	
Present	42 (23%)	23 (19%)	19 (30%)		32 (26%)	10 (16%)	
mGPS (n=96)				p=0.395			p=0.680
mGPS 0	39 (41%)	28 (44%)	11 (34%)		27 (40%)	14 (50%)	
mGPS 1	36 (38%)	24 (38%)	12 (38%)		25 (37%)	9 (32%)	
mGPS 2	21 (22%)	12 (20%)	9 (28%)		15 (22%)	5 (18%)	
CMS (n=155)				p=0.054			p=0.354
CMS1	16 (10%)	12 (12%)	4 (7%)		8 (8%)	8 (15%)	
CMS2/3	109 (70%)	75 (74%)	34 (63%)		73 (72%)	36 (68%)	
CMS4	30 (19%)	14 (14%)	16 (30%)		21 (21%)	9 (17%)	
CEA (n=155)				**p=0.029**			p=0.919
CEA-low	101 (65%)	**72 (71%)**	**29 (54%)**		70 (65%)	31 (65%)	
CEA-high	54 (35%)	**29 (29%)**	**25 (46%)**		37 (35%)	17 (35%)	
CA19-9 (n=135)				**p=0.035**			p=0.584
CA19-9-low	111 (82%)	**80 (87%)**	**31 (72%)**		77 (81%)	34 (85%)	
CA19-9-high	24 (18%)	**31 (13%)**	**28 (28%)**		19 (19%)	6 (15%)	

Table 4: The relationship between Glasgow microenvironment score (GMS) and clinicopathological parameters was assessed using Chi-squared test. Significant correlations were marked with bold font, while tendencies where p<0.1 were marked with italic font. In some cases, percentages do not add up to 100% precisely due to rounding. Abbreviations: mGPS – modified Glasgow Prognostic Score, CMS – consensus molecular subtypes, CEA – carcinoembryonic antigen, CA 19-9 – Carbohydrate antigen 19-9

Clinico-pathological features	All patients (n=185)	GMS (n=185)			
		GMS0 (n=102)	GMS1 (n=42)	GMS2 (n=41)	p value
Age					**p=0.008**
<65	65 (35%)	**26 (26%)**	**16 (38%)**	**23 (56%)**	
65-74	77 (42%)	**50 (49%)**	**14 (33%)**	**13 (32%)**	
75<	43 (23%)	**26 (26%)**	**12 (29%)**	**5 (12%)**	
Sex					p=0.904
Female	97 (52%)	52 (51%)	23 (55%)	22 (54%)	
Male	88 (48%)	50 (49%)	19 (45%)	19 (46%)	
Location					p=0.158
Right colon	75 (41%)	49 (48%)	13 (31%)	13 (32%)	
Left colon	58 (31%)	25 (25%)	17 (41%)	16 (39%)	
Rectum	52 (28%)	28 (28%)	12 (29%)	12 (29%)	
pT					**p=0.015**
pT1	2 (1%)	**2 (2%)**	**0 (0%)**	**0 (0%)**	
pT2	34 (18%)	**26 (26%)**	**6 (14%)**	**2 (5%)**	
pT3	134 (72%)	**70 (69%)**	**32 (76%)**	**32 (78%)**	
pT4	15 (8%)	**4 (4%)**	**4 (10%)**	**7 (17%)**	
pN (n=184)					**p=0.001**
pN0	82 (45%)	**56 (55%)**	**19 (46%)**	**7 (17%)**	
pN1	67 (36%)	**32 (31%)**	**14 (34%)**	**21 (51%)**	
pN2	35 (19%)	**14 (14%)**	**8 (20%)**	**13 (32%)**	
M					**p<0.001**
M0	143 (77%)	**89 (87%)**	**32 (76%)**	**22 (54%)**	
M1	42 (23%)	**13 (13%)**	**10 (24%)**	**19 (46%)**	
Stage					**p<0.001**
I	26 (14%)	**21 (21%)**	**4 (10%)**	**1 (2%)**	
II	48 (26%)	**30 (29%)**	**13 (31%)**	**5 (12%)**	
III	69 (37%)	**38 (37%)**	**15 (36%)**	**16 (39%)**	
IV	42 (23%)	**13 (13%)**	**10 (24%)**	**19 (46%)**	
Grade					p=0.718
Low/moderate	161 (87%)	90 (88%)	35 (83%)	36 (88%)	
High	24 (13%)	12 (12%)	7 (17%)	5 (12%)	
Lymphatic invasion					**p<0.001**
Not present	122 (66%)	**74 (73%)**	**32 (76%)**	**16 (39%)**	
Present	63 (34%)	**28 (28%)**	**10 (24%)**	**25 (61%)**	
Perineural invasion					**p=0.010**
Not present	170 (92%)	**97 (95%)**	**40 (95%)**	**33 (81%)**	
Present	15 (8%)	**5 (5%)**	**2 (5%)**	**8 (20%)**	
Vascular invasion					p=0.187
Not present	143 (77%)	37 (86%)	68 (77%)	38 (70%)	
Present	42 (23%)	6 (14%)	20 (23%)	16 (30%)	
mGPS (n=96)					p=0.316
mGPS 0	39 (41%)	25 (52%)	7 (33%)	9 (35%)	
mGPS 1	36 (38%)	16 (33%)	7 (33%)	11 (42%)	
mGPS 2	21 (22%)	7 (15%)	7 (33%)	6 (23%)	
CMS (n=155)					p=0.119
CMS1	16 (10%)	12 (14%)	1 (3%)	3 (8%)	
CMS2/3	109 (70%)	59 (69%)	28 (82%)	22 (61%)	
CMS4	30 (19%)	14 (17%)	5 (15%)	11 (37%)	
CEA (n=155)					p=0.215
CEA-low	101 (65%)	55 (68%)	25 (71%)	21 (54%)	
CEA-high	54 (35%)	26 (32%)	10 (29%)	18 (46%)	
CA19-9 (n=135)					**p=0.011**
CA19-9-low	111 (82%)	**62 (86%)**	**29 (91%)**	**20 (65%)**	
CA19-9-high	24 (18%)	**10 (14%)**	**3 (9%)**	**11 (36%)**	

APC was significantly elevated in males (p=0.003), associated with right-sidedness (p=0.013), CMS1 (p<0.001), showed significant association with lymphatic invasion (p=0.045) and there was a tendency towards distant metastasis (p=0.068) and vascular invasion (p=0.077). (Table 6, Figure 4).

The mGPS showed significant association with higher grade (p=0.042) and a tendency towards elevated pT (p=0.057) (Table 7). CEA was significantly lower in left sided tumors (p=0.033). Elevated CEA levels were associated with stage (p<0.001), pT (p=0.044) and distant metastasis (p<0.001) and also showed a tendency towards higher pN (p=0.062) (Table 6, Table 3 and Figure 6). CA19-9 was also associated with stage (p<0.001), pT (p=0.002), distant metastasis (p<0.001), lymphatic invasion (p=0.015), and GMS (p=0.027). There was a tendency towards vascular (p=0.065) and perineural (p=0.081) invasion (Table 6, Table 3, Figure 5).

CMS1 was significantly associated with right colonic localization (p=0.006) and higher histological grades (p<0.001). CMS4 was associated with higher stage (p=0.006), lymphatic and perineural invasion (p<0.001 and p=0.006, respectively) pN (p=0.001) and M (p=0.022) descriptors, and there was a tendency towards TSR-high just failing to be significant (p=0.054) (Table 7 and Figure 5). We did not find any significant correlation between the examined tumor markers (CEA and CA19-9) and CMS (p=0.439 and p=0.215) (Figure 5, Table 7).

4.4.Survival analysis

For TSR_{visual}, the 5-year OS for patients with TSR-high versus TSR-low was 49% versus 74% (p<0.001), and $TSR_{software}$ yielded similar results (TSR-high versus TSR-low: 50% vs 73%, p=0.02) (Table 8). On multivariate analysis both visual and software TSR (HR for TSR_{visual}: 1.781 (95% CI: 1.060-2.992, p=0.029); HR for $TSR_{software}$: 2.005 (95% CI:1.146-3.507, p=0.011) were found to be associated with poorer OS (Table 9).

Patients with high GMS (p=0.003), high ANC (p=0.007), low albumin (p=0.027), elevated CRP (p=0.006), elevated CEA (p<0.001) and CA19-9 (p<0.001), as well as higher mGPS (p=0.002) and mesenchymal subtype (CMS4) (p=0.049) had poorer overall survival (Table 8, Figure 7).

Apart from TSR, in the univariate Cox regression analysis GMS, mGPS, ANC, CRP, Albumin, CEA and CA19-9 were significantly associated with OS; CMS presented a tendency (with a p=0.055, just failing to be significant) towards increased risk of death in

CMS4 patients. In the multivariate analysis mGPS (p=0.003), Albumin (p=0.003), CRP (p=0.018), CA19-9 (p=0.013), and STM-score (p≤0.001) were significant predictors of OS (independent of sex, grade, stage and vascular invasion) (Table 9).

4.4.The STM-scoring system

In our research the strongest independent TME-based marker was TSRvisual (9). Also, CA19-9, a tumor marker often, though not routinely used in colorectal cancer follow up, came out as a predictor of overall survival in our analysis (Table 9). Incorporating these two, STM was created. The assessment of STM is described in Methods previously.

Cases classified as STM2 were associated with younger age (p=0.014), higher pN (p=0.033) and M (p<0.001), as well as higher TNM stage (p<0.001), and presence of lymphatic (p<0.001) and perineural invasion (p<0.001), and also with elevated CEA-levels (p=0.002) (Table 10). The mesenchymal subtype of CMS was also more prevalent in STM1 and STM2 groups (p=0.048) (Table 3). There was a tendency towards higher pT (p=0.071), also, preoperative serum CRP and CEA levels correlated with STM1 and STM2 (p=0.017 and p<0.001) (Table 10, Table 11).

The STM score significantly stratified 5-year overall survival (86% versus 54% versus 42%) with Kaplan-Meier analysis (Table 8). In the univariate Cox-regression analysis STM was significantly associated with OS (HR: 7.4 (3-18), p<0.001), and in the multivariate Cox-regression analysis STM was found to be an independent prognosticator of OS (independent of sex, grade, stage and vascular invasion (p<0.001, HR: 4.3 (1.5-12) (Table 9).

Table 6: The relationship between clinicopathological features and quantitative systemic inflammation-related markers and canonical tumor marker was examined using non-parametric tests (Mann-Whitney U-test and Kruskal-Wallis H-test). Significant relations were marked with bold font, tendencies where p<0.1 were marked with italic font. Numbers shown in parentheses denote median values of each continuous variable within the respective categorical variable group. Abbreviations: CRP – C reactive protein, ANC – absolute neutrophil count, ALC – absolute lymphocyte count, APC, absolute platelet count, NLR – neutrophil-lymphocyte ratio, PLR – platelet-lymphocyte ratio, CEA – carcinoembryonic antigen, CA 19-9 – carbohydrate antigen 19-9, CMS – consensus molecular subtype, dMMR – mismatch repair deficient, TSR – tumor-stroma ratio, KM grade – Klintrup-Makinen grade, GMS – Glasgow microenvironment score.

Clinico-pathological features	Albumin (n=107)	CRP (n=149)	ANC (n=170)	ALC (n=170)	APC (n=180)	CEA (n=155)	CA19-9 (n=135)
Age	**p=0.039**	p=0.986	p=0.199	**p=0.007**	p=0.816	p=0.850	p=0.639
<65	**(42)**	(12.2)	(4.87)	**(1.6)**	(263)	(8.8)	(118)
65-74	**(41.5)**	(4.3)	(4.84)	**(1.6)**	(250)	(2.1)	(17)
75<	**(38.6)**	(7.7)	(4.54)	**(1.41)**	(242)	(3.3)	(11.4)
Sex	p=0.215	p=0.732	p=0.528	p=0.585	**p=0.003**	*p=0.099*	p=0.513
Female	(41.2)	(6.1)	(4.7)	(1.63)	**(236)**	*(3.3)*	(13.6)
Male	(40.9)	(7.7)	(4.9)	(1.54)	**(278)**	*(2.6)*	(20.5)
Location	p=0.338	p=0.338	p=0.978	p=0.628	**p=0.013**	**p=0.033**	p=0.131
Right colon	(39.8)	(9.7)	(4.8)	(1.6)	**(317)**	**(2.9)**	(14.4)
Left colon	(41.8)	(3.3)	(4.8)	(1.7)	**(250)**	**(2.5)**	(26.1)
Rectum	(41.1)	(5)	(4.7)	(1.3)	**(237)**	**(3.5)**	(17.2)
pT	p=0.241	**p<0.001**	**p=0.011**	p=0.901	p=0.459	**p=0.044**	**p=0.002**
pT1	(40.1)	**(7.1)**	**(3.5)**	(1.4)	(270)	**(1.8)**	**(21)**
pT2	(42.6)	**(5.1)**	**(4.8)**	(1.7)	(278)	**(2.1)**	**(4.8)**
pT3	(40.4)	**(5.5)**	**(4.7)**	(1.5)	(244)	**(3.6)**	**(18)**
pT4	(41.4)	**(87.7)**	**(6.1)**	(1.7)	(293)	**(2.6)**	**(31)**
pN	p=0.509	p=0.354	*p=0.058*	p=0.145	p=0.333	*p=0.062*	p=0.179
pN0	(41)	(4.5)	*(4.6)*	(1.3)	(250)	*(2.3)*	(18)
pN1	(41)	(9.1)	*(4.9)*	(1.7)	(237)	*(3.5)*	(14)
pN2	(40)	(9.8)	*(6.1)*	(1.7)	(308)	*(2.9)*	(20)
M	p=0.895	**p=0.007**	p=0.457	p=0.800	*p=0.068*	**p<0.001**	**p<0.001**
M0	(41)	**(5)**	(4.7)	(1.6)	*(250)*	**(2.2)**	**(11)**
M1	(40)	**(13)**	(4.9)	(1.6)	*(274)*	**(9.5)**	**(78)**
Stage	*p=0.089*	**p=0.002**	p=0.111	p=0.213	p=0.293	**p<0.001**	**p<0.001**
I	*(42)*	**(4.3)**	(4.7)	(1.5)	(278)	**(1.6)**	**(12)**
II	*(41)*	**(4)**	(4.6)	(1.2)	(231)	**(2.3)**	**(17)**
III	*(41)*	**(6)**	(5.2)	(1.8)	(263)	**(3.1)**	**(9.6)**
IV	*(40)*	**(13)**	(4.9)	(1.6)	(274)	**(9.5)**	**(78)**
Grade	p=0.579	**p=0.027**	p=0.288	p=0.906	p=0.220	p=0.877	p=0.812
Low/moderate	(41)	**(6.1)**	(4.8)	(1.6)	(248)	(3.4)	(18)
High	(41)	**(7.7)**	(5.8)	(1.6)	(302)	(2.6)	(9.1)
Lymphatic invasion	p=0.543	**p=0.032**	p=0.398	p=0.548	**p=0.045**	p=0.262	**p=0.015**
Not present	(41)	**(4.3)**	(4.6)	(1.5)	**(242)**	(2.9)	**(17)**
Present	(40)	**(12)**	(6.1)	(1.6)	**(315)**	(3.4)	**(21)**
Perineural invasion	p=0.992	*p=0.063*	p=0.847	p=0.708	p=0.228	p=0.198	*p=0.081*
Not present	(41)	*(5.2)*	(4.7)	(1.6)	(248)	(2.8)	*(17)*
Present	(40)	*(12)*	(6.3)	(1.7)	(263)	(8.8)	*(140)*
Vascular invasion	p=0.247	**p=0.026**	p=0.424	p=0.187	*p=0.077*	p=0.255	*p=0.065*
Not present	(41)	**(4.7)**	(4.6)	(1.6)	*(248)*	(2.5)	*(14)*
Present	(39)	**(21)**	(6.3)	(1.5)	*(307)*	(3.3)	*(21)*

CMS (n=155) dMMR Epithelial Mesenchymal	p=0.801 (43) (41) (40)	p=0.342 (11) (4.7) (8.6)	p=0.501 (5.9) (4.6) (5)	p=0.512 (1.6) (1.3) (1.7)	**p<0.001** **(490)** **(232)** **(315)**	p=0.483 (2) (2.9) (3.4)	p=0.357 (12) (18) (11)
TSR TSR-low TSR-high	p=0.523 (41) (41)	p=0.256 (4.3) (9.1)	p=0.138 (4.6) (6)	p=0.171 (1.4) (1.7)	p=0.809 (250) (272)	*p=0.062* *(2.4)* *(6)*	*p=0.072* *(12)* *(27)*
KM grade KM-low KM-high	p=0.606 (41) (41)	p=0.386 (7.7) (4.3)	p=0.206 (4.9) (4.5)	p=0.939 (1.7) (1.3)	p=0.524 (254) (274)	p=0.906 (2.6) (3.5)	p=0.782 (7.2) (18)
GMS GMS 0 GMS 1 GMS 2	p=0.163 (42) (38) (40)	p=0.409 (4.3) (2.8) (19)	p=0.270 (4.6) (4.7) (6.2)	p=0.164 (1.6) (1.3) (1.8)	p=0.393 (274) (227) (291)	p=0.602 (2.6) (2.2) (4.9)	**p=0.027** **(17)** **(5.5)** **(25)**

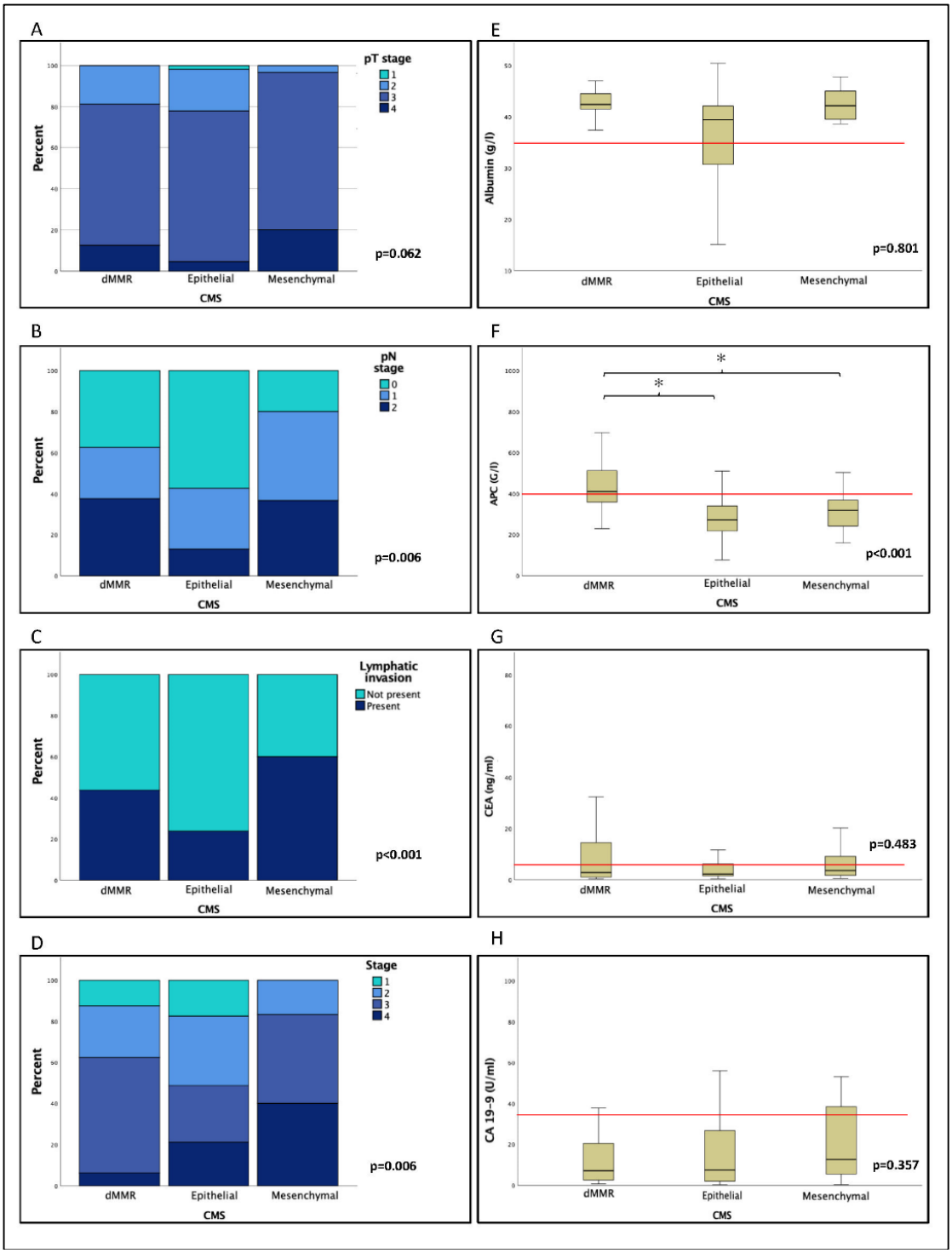

Figure 5: The relationship of CMS and clinicopathological features was analysed using Chi-square test (A-D). Mesenchymal subtype was associated with higher pT, pN, and stage and presence of lymphatic invasion. The relationship of CMS and systemic markers was assessed using non-parametric Mann-Whitney and Kruskal-Wallis test (E-H). Preoperative absolute platelet count was significantly elevated in dMMR tumors. Tumor markers were not significantly associated with CMS. The horizontal red line represents cut off values. ✲ marks significant associations, $p<0.05$. Abbreviations: dMMR – Mismatch repair deficient, CMS – consensus molecular subtypes, APC – absolute platelet count, CEA – carcinoembryonic antigen, CA 19-9 – carbohydrate antigen 19-9.

Table 7: The relationship between consensus molceular subtypes and clinicopathological parameters was assessed using Chi-squared test. Significant correlations were marked with bold font, while tendencies where p<0.1 were marked with italic font. In some cases, percentages do not add up to 100% precisely due to rounding. Abbreviations: CMS – consensus molecular subtypes, mGPS – modified Glasgow Prognostic Score, CEA – carcinoembryonic antigen, CA 19-9 – Carbohydrate antigen 19-9

Clinico-pathological parameters	All patients (n=185*)	CMS (n=155)			
		CMS1 (n=16)	CMS2/3 (n=109)	CMS4 (n=30)	p value
Age (n=185)					p=0.883
<65	65 (35%)	4 (25%)	35 (32%)	12 (40%)	
65-74	77 (42%)	8 (50%)	49 (45%)	12 (40%)	
75<	43 (23%)	4 (25%)	25 (23%)	6 (20%)	
Sex (n=185)					p=0.337
Female	97 (52%)	6 (38%)	59 (54%)	18 (60%)	
Male	88 (48%)	10 (63%)	50 (46%)	12 (40%)	
Location (n=185)					**p=0.006**
Right colon	75 (41%)	**13 (81%)**	**37 (34%)**	**13 (43%)**	
Left colon	58 (31%)	**2 (13%)**	**36 (33%)**	**11 (37%)**	
Rectum	52 (28%)	**1 (6%)**	**36 (33%)**	**6 (20%)**	
pT (n=185)					*p=0.062*
pT1	2 (1%)	0 (0%)	2 (2%)	0 (0%)	
pT2	34 (18%)	3 (19%)	22 (20%)	1 (3%)	
pT3	134 (72%)	11 (69%)	80 (73%)	23 (77%)	
pT4	15 (8%)	2 (13%)	5 (5%)	6 (20%)	
pN (n=184)					**p=0.001**
pN0	82 (45%)	**6 (38%)**	**62 (57%)**	**6 (20%)**	
pN1	67 (36%)	**4 (25%)**	**32 (30%)**	**13 (43%)**	
pN2	35 (19%)	**6 (38%)**	**14 (13%)**	**11 (37%)**	
M (n=185)					**p=0.022**
M0	143 (77%)	**15 (94%)**	**86 (79%)**	**18 (60%)**	
M1	42 (23%)	**1 (6%)**	**23 (21%)**	**12 (40%)**	
Stage (n=185)					**p=0.006**
I	26 (14%)	**2 (13%)**	**9 (17%)**	**0 (0%)**	
II	48 (26%)	**4 (25%)**	**37 (34%)**	**5 (17%)**	
III	69 (37%)	**9 (56%)**	**30 (28%)**	**13 (43%)**	
IV	42 (23%)	**1 (6%)**	**23 (21%)**	**12 (40%)**	
Grade (n=185)					**p<0.001**
Low/moderate	161 (87%)	**9 (56%)**	**100 (92%)**	**24 (80%)**	
High	24 (13%)	**7 (44%)**	**9 (8%)**	**6 (20%)**	
Lymphatic invasion (n=185)					**p<0.001**
Not present	122 (66%)	**9 (56%)**	**83 (86%)**	**12 (40%)**	
Present	63 (34%)	**7 (44%)**	**26 (24%)**	**18 (60%)**	
Perineural invasion (n=185)					**p=0.006**
Not present	170 (92%)	**14 (88%)**	**104 (95%)**	**26 (77%)**	
Present	15 (8%)	**2 (13%)**	**5 (5%)**	**7 (23%)**	
Vascular invasion (n=185)					p=0.858
Not present	143 (77%)	12 (75%)	82 (75%)	24 (80%)	
Present	42 (23%)	4 (25%)	27 (25%)	6 (20%)	
mGPS (n=96)					p=0.486
mGPS 0	39 (41%)	2 (40%)	24 (44%)	10 (56%)	
mGPS 1	36 (38%)	3 (60%)	17 (31%)	5 (28%)	
mGPS 2	21 (22%)	0 (0%)	14 (26%)	3 (17%)	
CEA (n=155)					p=0.439
CEA-low	101 (65%)	7 (58%)	62 (70%)	15 (58%)	
CEA-high	54 (35%)	4 (42%)	27 (30%)	11 (42%)	
CA19-9 (n=135)					p=0.215
CA19-9-low	111 (82%)	12 (100%)	63 (84%)	17 (77%)	
CA19-9-high	24 (18%)	0 (0%)	12 (16%)	5 (23%)	

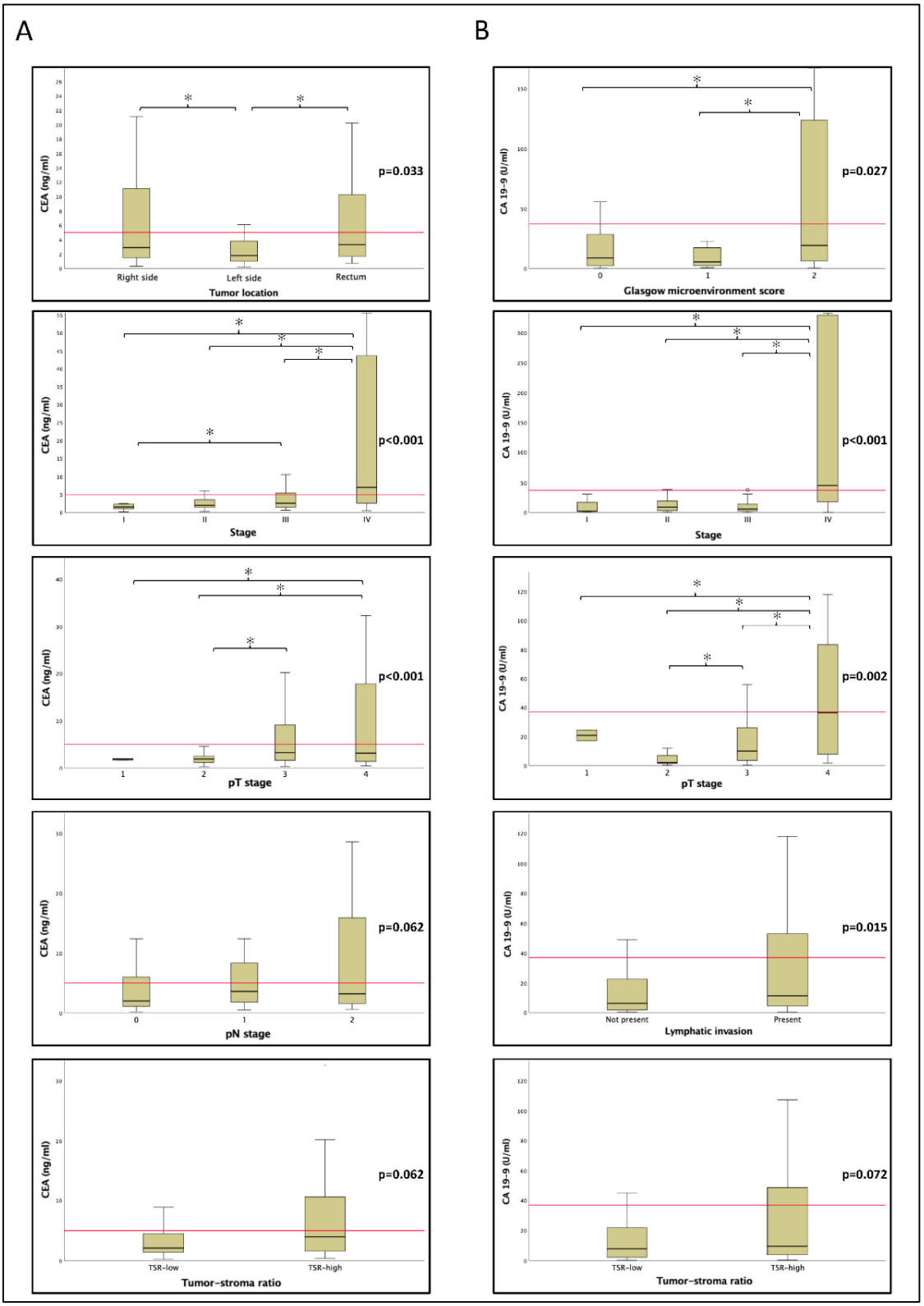

Figure 6: The relationship between tumor markers CEA (A) and CA 19-9 (B) and clinicopathological features. Elevated tumor marker levels were mostly associated with adverse features. There was a tendency between tumor markers and high tumor-stroma ratio (TSR). The horizontal red line represents cut off value. Abbreviations: CEA – carcinoembryonic antigen, CA 19-9 – carbohydrate antigen 19-9, TSR – tumor-stroma ratio. ✲ marks significant associations, p<0.05.

Table 8: The relationship between TME, SIR markers, CMS and survival parameters. Abbreviations: OS – overall survival, LRFS – local relapse free survival, DMFS – distant metastasis free survival, TSR – tumor-stroma ratio, KM grade – Klintrup-Makinen grade, GMS – Glasgow microenvironment score, CMS – consensus molecular subtype, ANC – absolute neutrophil count, ALC – absolute lymphocyte count, APC – absolute platelet count, NLR – neutrophil-lymphocyte ratio, PLR – platelet-lymphocyte ratio, NPS – neutrophil platelet sore, mGPS – modified Glasgow prognostic score, CRP – C reactive protein, CEA – carcinoembryonic antigen, CA 19-9 – carbohydrate antigen 19-9, STM – stroma- tumor marker score

	5 year OS, stage I-IV (median survival)	p value
TSRvisual (n=185)	**TSR-low: 74%** **TSR-high: 49%**	**p<0.001**
TSRsoftware (n=185)	**TSR-low: 73%** **TSR-high: 50%**	**p=0.02**
KM grade (n=185)	KM low: 67% KM high: 62%	p=0.763
GMS (n=185)	**GMS 0: 70%** **GMS 1: 68%** **GMS 2: 48%**	**p=0.003**
CMS (n=155)	**dMMR: 73%** **Epithelial: 72%** **Mesenchymal: 50%**	**p=0.049**
CEA (n=155)	**CEA low: 80%** **CEA high: 43%**	**p<0.001**
CA 19-9 (n=135)	**CA 19-9 low: 76%** **CA 19-9 high: 0%**	**p<0.001**
mGPS (n=95)	**mGPS 0: 83%** **mGPS 1: 59%** **mGPS 2: 38%**	**p=0.002**
CRP (n=149)	**CRP low: 73%** **CRP high: 55%**	**p=0.007**
Albumin (n=107)	**Albumin low: 51%** **Albumin high: 73%**	**p=0.027**
ANC (n=170)	**ANC low: 81%** **ANC high: 56%**	**p=0.006**
ALC (n=170)	ALC low: 63% ALC high: 70%	p=0.444
APC (n=180)	APC low: 70% APC high: 60%	p=0.398
STM (n=135)	**STM0: 86%** **STM1: 54%** **STM2: 42%**	**p<0.001**

*Table 9: Results of uni- and multivariate Cox regression analysis regarding overall survival *: all variables were assessed individually in a multivariate analysis including sex, stage, grade and vascular invasion using enter method. Abbreviations: TSR – tumor-stroma ratio, KM grade – Klintrup-Makinen grade, GMS – Glasgow microenvironment score, CMS – consensus molecular subtype, dMMR – mismatch repair deficient, ANC – absolute neutrophil count, ALC – absolute lymphocyte count, mGPS – modified Glasgow prognostic score, CRP – C reactive protein, CEA – carcinoembryonic antigen, CA 19-9 – carbohydrate antigen 19-9, STM – Stroma-Tumor Marker score, HR – hazard ratio, CI – confidence interval*

	Univariate analysis for OS HR (95% CI)	p-value	Multivariate analysis for OS HR (95% CI)*	p-value
TSR visual (low/high)	**2.7 (1.6-44)**	**<0.001**	**1.8 (1.1-3)**	**0.029**
TSR software (low/high)	**2.3 (1.3-4)**	**0.003**	**2 (1.1-3.5)**	**0.011**
KM grade (low/high)	1.1 (0.6-1.8)	0.763	-	-
GMS (0/1/2)	**2.3 (1.3-4)**	**0.004**	1.4 (0.8-2.6)	0.130
CMS (dMMR/ Epithelial/ Mesenchymal)	*2.2 (0.6-6.8)*	*0.055*	1.7 (0.5-5.4)	0.371
ANC (low/high)	**2.1 (1.3-3.6)**	**0.007**	*1.7 (0.99-3)*	*0.055*
ALC (low/high)	0.8 (0.5-1.4)	0.445	-	-
APC (low/high)	1.3 (0.7-2.4)	0.399	-	-
mGPS (0/1/2)	**4.8 (1.9-12)**	**0.004**	**5.6 (2.1-15)**	**0.003**
Albumin (low/high)	**0.5 (0.3-0.9)**	**0.030**	**0.5 (0.2-0.9)**	**0.022**
CRP (low/high)	**2 (1.2-3.5)**	**0.008**	**1.9 (1.1-3.4)**	**0.018**
CEA (low/high)	**2.9 (1.7-5.2)**	**<0.001**	*1.7 (0.9-3.3)*	*0.087*
CA 19-9 (low/high)	**3.9 (2-7.5)**	**<0.001**	**2.8 (1.2-6.1)**	**0.013**
STM score (0/1/2)	**7.4 (3-18)**	**<0.001**	**4.3 (1.6-11.9)**	**<0.001**

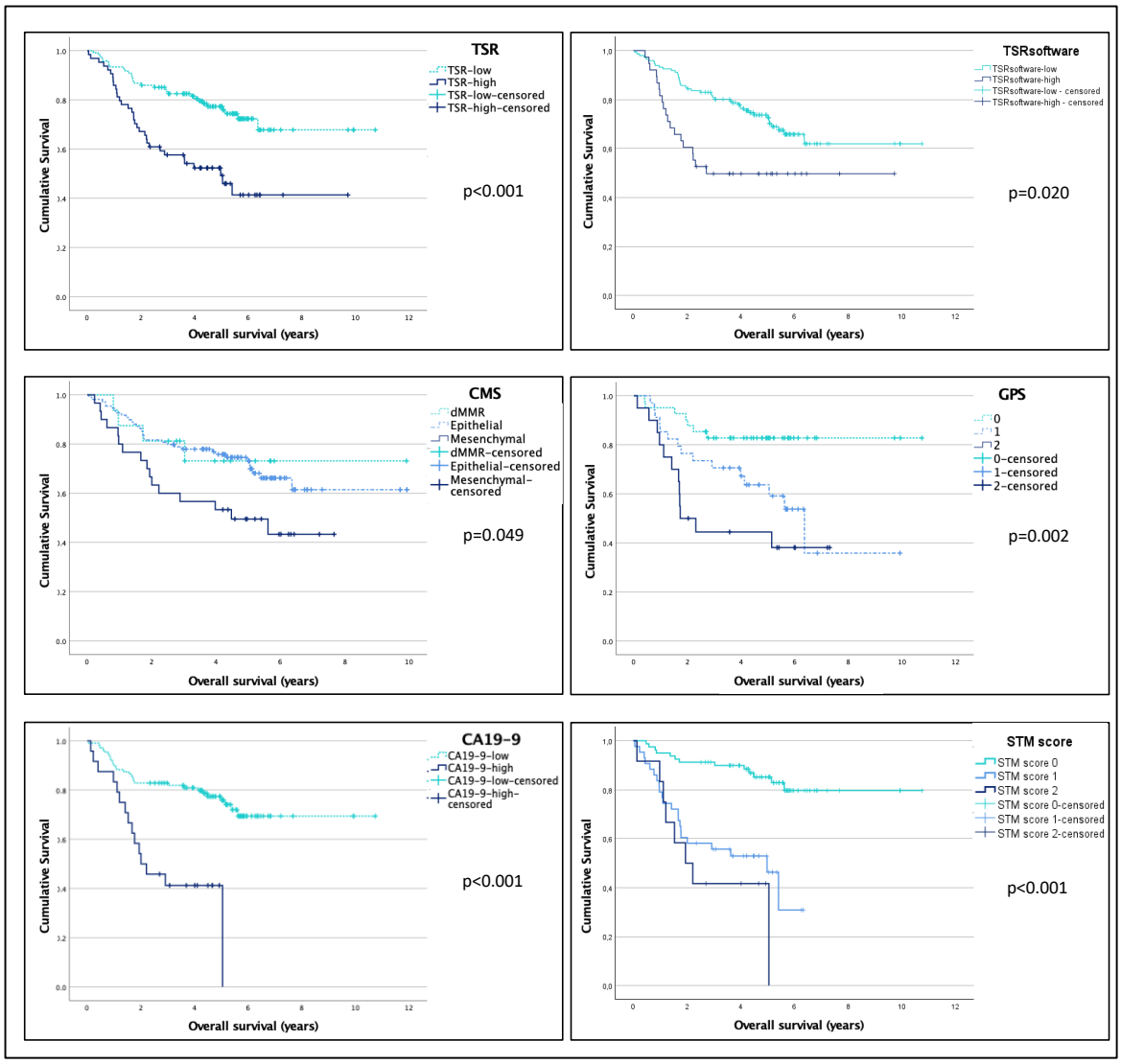

Figure 7: The effect of microenviromental and systemic markers on overall survival (OS). Abbreviations: TSR – tumor stroma ratio, TSRsoftware – software assisted tumor stroma ratio, , CMS – consensus molecular subtype, mGPS – modified Glasgow Prognostic Score, CA19-9 – carbohydrate antigen 19-9, STM score – Stroma-Tumor Marker Score

Table 10: The relationship between stroma-tumor marker (STM) score and clinicopathological features. The relationship between stroma-tumor marker (STM) score and clinicopathological features was assessed using Chi-squared test. Significant correlations were marked with bold font, while tendencies where p<0.1 were marked with italic font. Abbreviations: STM – stroma-tumor marker score, CMS – consensus molecular subtype, dMMR – mismatch repair deficient, mGPS – modified Glasgow prognostic score, CEA – carcinoembryonic antigen.

Clinico-pathological features	All patients (n=135)	Stroma-tumor marker (STM) score			
		STM 0 (n=80)	STM 1 (n=43)	STM 2 (n=12)	p value
Age					**0.014**
<65	46 (34%)	21 (26%)	16 (37%)	9 (75%)	
65-74	60 (44%)	42 (53%)	16 (37%)	2 (17%)	
75<	29 (22%)	17 (21%)	11 (26%)	1 (8%)	
Sex					0.877
Female	73 (54%)	44 (55%)	22 (51%)	7 (58%)	
Male	62 (46%)	36 (45%)	21 (49%)	5 (42%)	
Location					0.288
Right colon	57 (42%)	36 (45%)	16 (37%)	5 (42%)	
Left colon	44 (33%)	26 (33%)	12 (28%)	6 (50%)	
Rectum	34 (25%)	18 (23%)	15 (35%)	1 (8%)	
pT					*0.071*
pT1	2 (1.5%)	*2 (3%)*	*0 (0%)*	*0 (0%)*	
pT2	25 (19%)	*20 (25%)*	*5 (12%)*	*0(0%)*	
pT3	97 (72%)	*55 (69%)*	*32 (74%)*	*10 (83%)*	
pT4	11 (8%)	*3 (4%)*	*6 (14%)*	*2 (17%)*	
pN					**0.033**
pN0	58 (43%)	**41 (52%)**	**16 (37%)**	**1 (8%)**	
pN1	51 (38%)	**27 (34%)**	**18 (42%)**	**6 (50%)**	
pN2	25 (19%)	**11 (14%)**	**9 (21%)**	**5 (42%)**	
M					**<0.001**
M0	104 (77%)	**73 (91%)**	**28 (65%)**	**3 (25%)**	
M1	31 (23%)	**7 (9%)**	**15 (35%)**	**9(75%)**	
Stage					**<0.001**
I	21 (16%)	**17 (23%)**	**4 (9%)**	**0 (0%)**	
II	30 (22%)	**22 (28%)**	**8 (19%)**	**0 (0%)**	
III	53 (39%)	**34 (43%)**	**16 (37%)**	**3 (25%)**	
IV	31 (23%)	**7 (9%)**	**15 (35%)**	**9 (75%)**	
Grade					0.916
Low/moderate	119 (88%)	70 (88%)	38 (88%)	11 (92%)	
High	19 (12%)	10 (13%)	5 (12%)	1 (8%)	
Lymphatic invasion					**<0.001**
Not present	89 (64%)	**62 (78%)**	**20 (47%)**	**4 (33%)**	
Present	49 (36%)	**18 (23%)**	**23 (54%)**	**8 (67%)**	
Perineural invasion					**0.001**
Not present	121(90%)	**78 (98%)**	**34 (79%)**	**9 (75%)**	
Present	14 (10%)	**2 (3%)**	**9 (21%)**	**3 (25%)**	
Vascular invasion					0.440
Not present	103 (76%)	64 (80%)	31 (72%)	8 (67%)	
Present	32 (24%)	16 (20%)	12 (28%)	4 (33%)	
CMS					**0.048**
dMMR	12 (11%)	10 (15%)	2 (6%)	0 (0%)	
Epithelial	75 (69%)	48 (73%)	20 (59%)	7 (78%)	
Mesenchymal	22 (20%)	8 (12%)	12 (25%)	2 (22%)	
mGPS					0.414
mGPS 0	37 (50%)	24 (60%)	9 (39%)	4 (36%)	
mGPS 1	26 (35%)	12 (30%)	9 (39%)	5 (46%)	
mGPS 2	11 (15%)	4 (10%)	5 (22%)	2 (18%)	
CEA (n=152)					**0.002**
CEA-low	90 (67%)	62 (78%)	24 (56%)	4 (33%)	
CEA-high	45 (33%)	18 (23%)	19 (44%)	8 (67%)	

Table 11: The relationship between stroma-tumor marker (STM) score and systemic inflammatory response. The relationship STM and systemic inflammatory response related markers and CEA were evaluated using the non-parametric Kruskal-Wallis H test. Significant variables were marked with bold font, tendencies where p<0.1 were marked with italic font. Abbreviations: STM – stroma-tumor maker score, CEA – carcioembryonic antigen, CRP – C reactive protein, ANC – absolute neutrophil count, ALC – absolute lymphocyte count, APC, absolute platelet count.

	Number of patients	STM 0 (mean rank)	STM 1 (mean rank)	STM 2 (mean rank)	p value
CEA	135	58.97	75.56	101.13	**<0.001**
CRP	114	49.97	68.38	66.28	**0.017**
Albumin	82	45.98	36.20	34.82	0.115
ANC	127	60.15	69.93	67.27	0.370
ALC	127	65.94	62.54	56.55	0.697
APC	134	64.91	73.74	62.21	0.430

5. Discussion

5.1. TSR_{visual} and $TSR_{software}$

Similarly to previous studies (12-14), stroma-high tumors, assessed by either method, represented an agressive phenotype with poor prognosis and inferior survival in this cohort. Agreement between observers (κ=0.778) is concordant to previous findings (12, 43, 44), however, the agreement between $TSR_{software}$ and TSR_{visual} is lower (κ=0.472) compared to Geesink et al's (κ=0.521) and Li et al's (κ=0.813) work (33, 37, 38). Also, the software performance was somewhat limited compared to previous AI-based studies. For comparison, others showed a remarkable 90% to 94.6% accuracy (33, 37) and implied strong correlation and high agreement between software-assisted and annotated TSR (38), while our results yieleded an accuracy of 80% regarding tumor epithel, and 72.4% regarding stromal content estimation. These results demonstrate moderate to good performance, which might be explained with the lower number of annotations used for training pattern recognition (in our study only 10 annotations per tissue type could be made, while in CNN-based datasets thousands of annotation are available per tissue type). Our experience was that even though software performance was somewhat lower compared to deep learning-based systems, still it proved to be a simple method with robust prognostic power. With further software optimalization to improve accuracy, a similar, user-friendly platform could be anticipated in routine diagnostics, though always just as aid to pathologists, not as replacement.

5.2. TME

According to literature data, higher KM grade is associated with favorable clinicopathological features (9, 45), which was the case in our study as well, though a significant association with OS wasn't observed. Although KM grade was described to be related to systemic inflammation (46), this finding was not confirmed in our study. Similarly to TSR, GMS also successfully stratified patients´ characteristics and survival, in agreement with preceding results (47). In conclusion, the aformentioned and easily assessible descriptors, TSR, KM-grade and GMS, can guide clinicians in CRC-prognostication.

5.3. SIR

The pre-operative systemic inflammation can be described using a variety of SIR markers (Suppl. Table 1). As described in previous reports (24, 48), some of the SIR markers were

associated with poor patient outcomes in this cohort as well. Three of them (CRP, albumin, mGPS) even came out as independent factors of overall survival. Among these markers CRP not only delivered robust prognostic power, but was also associated with adverse histological features and advanced stages. These results suggest that CRP represented the effect of inflammatory response on clinical outcome the most, which is not surprising, as CRP is a key acute phase protein of inflammatory processes (49).

Another substantial finding regarding SIR markers was that APC elevation correlated with right sidedness, and interestingly, in male patients. Elevation of APC was previously observed in dMMR CRC (46), which happened to be a subtype with higher prevalence in the right colon. This might give a potential explanation to our findings. Interestingly, women generally tend to have higher APC than men (50), which contradicts to our findings. It is also understood that higher APC is associated with poorer survival in CRC patients (51), but we haven't find such correlation in our cohort. The survival of dMMR patients are favourable in the early stages(18), however, metastatic dMMR patients without immun checkpoint inhibitor treatment have poor outcome(52). In our cohort, only 1 dMMR patient had distant metastasis, and the dMMR patients had superior survival compared to other subtypes. This seems to contradict the prognostic relevance of APC in this subgroup of patients, however, the association between dMMR tumors and APC is poorly understood. Furthermore, the small sample size might biased our results.

5.4.Tumor markers

Tumor markers CEA and CA19-9 and their relationship with TME and SIR was also assessed. In concordance with previous articles (53, 54), our study also showed that both CEA and CA19-9 were linked to advanced stages of CRC and CA19-9 even emerged as an independent factor of OS.

Surprisingly, both CEA and CA19-9 showed a statistically significant association with TSR, but not with KM grade and CMS, which is not yet reported elsewhere. The connection between TSR-high tumors and elevated tumor markers could be attributed to the higher presence of distant metastasis or locally advanced disease indicated by both markers.

5.5.STM

Important to point out, that both TSR and CA19-9 delivered strong prognostic value, which proposes a possible combined score, the STM, that bears similar or even stronger

prognostic power than these two variables separately (Table 9). As a matter of fact, STM was strongly associated with dismal clinicopathological parameters and proved to be the second best prognosticator of OS after tumor stage. In conclusion, combined scores based on histopathological features and routine laboratory tests, like mGPS or STM, could help identify a subset of CRC patients with higher risk of death or recurrence in a cost-effective and time sparing manner.

5.6.CMS

Reportedly, our study is the first one to assess the connection between CMS and SIR markers. CMS1 displays a characteristic inflammatory infiltrate that could lead to systemic inflammation which may be reflected in elevated SIR markers(46). In our analysis, CMS1 was associated with right-sidedness and elevated APC, similarly to previous findings (22)..

It is understood that CMS4 is associated with EMT-like gene expression profile and stromal infiltration signature (4), complement components and immunosuppressive chemokines (16). This signature is similar to wound healing responses or chronic, ineffective inflammation, where platelets are the first responders and several mediators present in CMS4 tumors are linked to platelet activation (55), hence an elevated APC was expected amongst mesenchymal CRCs. Interestingly, CMS4 tumors didn't exhibit elevation of any platelet-related, nor any other SIR markers in our cohort. In conclusion, no significant association between CMS and inflammation or SIR was found except for the elevation of APC in CMS1.

A recent paper(56) emphasizes the diversity of immunological subtypes and their distribution within CMS, that might provide an explanation as to why there is a lack of distinct SIR-related characteristic of each molecular subtype. Surprisingly, this research associates CMS2 (also, most epithelial-like CRCs) with a dominant wound healing-like immune response, while in CMS4 tumors with such an immunological profile are less frequent (56), which is contradictory with the previously mentioned report (55). Apparently, the rationale and exact mechanisms behind the resemblance of SIR-profiles of CMS-classified tumors are to be further examined.

Our study assigned poorer survival and higher TNM-stages to CMS4-tumors, which is similar to literature data (4, 57). Advanced CRCs are enriched in CMS4 (57), as was the case in our research. A possible pitfall of CMS classification could be the intratumoral

heterogeneity and EMT, especially if samples derive from the invasive front of the tumor, which can lead to misclassifying cases as CMS4 (58). To avoid sampling bias, our TMA cores were selected from the tumor centre. As of now, it is still difficult to answer based on current literature, whether CMS4 is the cause or the consequence of advanced CRCs. A study on exploring the relationship between interval CRC and CMS, as well as CMS subtyping of precursor lesions, or more precise studies dealing with heterogeneity within tumor areas (eg: multiple sampling from more tumor areas) could answer these questions Additionally, no significant association between traditional tumor markers and CMS was found in this research. Another article found that in stage III CMS4 CRCs , elevated CEA was associated with exceptionally poor prognosis, and suppressed tumor immunity was also observed in this subgroup (59). Similar analysis couldn't be performed in our database, as there were only 11 stage III CMS4 cases.

5.7.Limitations

A probable limitation of our study was the relatively small cohort size sometimes resulting few cases in the subclasses (especially for CMS4) and thus weak to moderate statistical power in these subgroups, as well as the retrospective nature with inclusion of stage IV patients. In addition, the IHC-based approach, a simple and cost-effective method, used for CMS classification, presents 87% of concordance with the gold-standard gene-expression based profiling, and does not differentiate between CMS2 and CMS3 subgroups(41, 42).

6. Conclusions

In conclusion, our results are in line with the literature data claiming that most TME, SIR markers and elevated CEA or CA19-9 are associated with adverse histological features and patient outcome. Our study approach broadens the potential options of cost-effective, evidence based prognostic tools, while implicating the utility of an accessible ML-based software as an aid in quantitative histological analysis. Although there is room for improvement in this field, it might be likely that similar tools would be used in the foreseeable future. In our view, even with forthcoming advancements, AI alone is not expected to take over the expertise and decisiveness of a qualified pathologist, but is more likely to assist them in simple, yet extensive tasks requiring precise estimations.

Assessing and combining routine histopathology (TSR) with laboratory findings (CA19-9) resulted in a novel, robust prognostic score, the STM score, which could be a simple and easily accessible risk stratificator. The authors believe this could be useful in identifying CRC patients at higher risk of recurrence or disease progression.

As in previous studies, CMS4 tumors represented an aggressive phenotype of CRC with adverse histological features and poor patient outcome, which was also reflected by its association with higher TSR. This further confirms the versatility of TSR assessment and its potential role in identifying patients at risk or cases with high probability of CMS4.

Up to now only very few studies investigated the connection between CMS and TME, SIR and tumor markers. Contrary to the authors' expectations, CMS4 and CMS2/3 were neither associated with any SIR nor tumor markers, only dMMR tumors correlated with plateled derived SIR markers, as described previously. This underlines the complexity of tumor-host response and proposes possible future investigations of this matter.

7. Summary

The subject of this thesis was the host reaction against malignancy in CRC patients in relation to one of the latest advancements, the CMS. The descriptors of host response in this article were markers of the TME and SIR, and additionally, their relation to tumor markers were examined as well.

Of exceptional focus was the TSR amongst TME markers, as it had proven to be one of the most robust, yet convenient HE-based prognosticators. Using a ML-based digital image analysis platform, the PatternQuant, $TSR_{software}$ delivered similar prognostic power as TSR_{visual} while presenting acceptable accuracy and inter rater agreement (Figure 8.a.). TSRvisual helped identifiyfing a subset of CRC patients with rather aggressive phenotype and poor outcome, and was also significantly associated with elevated levels of CEA and CA19-9 tumor markers and with CMS4, which was concordant with previous studies (Figure 8.b.). The KM grade was also associated with more advanced stage, however, it didn't yield significant prognostic power (Figure 8.b.). The combination of KM and TSR, the GMS score, was similarly associated with adverse clinicopathological features and poorer survival (Figure 8.b.).

Amongst SIR markers, elevated serum CRP outstandingly identified cases with adverse histopathological features (stage, lymphatic and vascular invasion) while also being an independent predictor of OS, however, it wasn't associated with any of the TME markers, nor CMS. The mGPS, a combined SIR marker comprising of CRP and albumin also reflected similar associations (Figure 8.b.). Out of the SIR markers, only elevated APC was associated with CMS1, while also showing tendency towards advanced disease (Figure 8.b. and c.).

Strikingly, the authors couldn't find significant connection between the TME and SIR, which had been expected based on preceding results.

The elevation of CEA and CA19-9 tumor markers also indicated advanced disease and poor outcome (Figure 8.b.). Utilising the combination of the most robust TME marker, the TSR and CA19.9, resulted in the STM-score, which stratified the outcome of CRC patients significantly and came out as an independent predictor of OS in the multivariate analysis, while also identifying a group of patients with adverse clinicopathological charateristics (Figure 8.d.).

For CMS classification a simplified and validated IHC-based method was applied. The CMS4 a.k.a. mesenchymal subtype represented an immensely adverse phenotype of CRC while showing weak correlation with TSR (Figure 8.c.). CMS1 tumors were also associated with right-sidedness and higher histological grade (Figure 8.c.). Remarkably, none of the CMSs were significantly associated with SIR or tumor markers. CMS4 showed a tendency towards poorer outcome, however, CMS didn't yield considerable prognostic value in our study.

Taken together, our study could not reveal a significant connection between CMS and host repsonse, still, both characteristics can help anticipating disease outcome and clinical decision making by distinguishing individuals who require closer follow up or vigorous treatment.

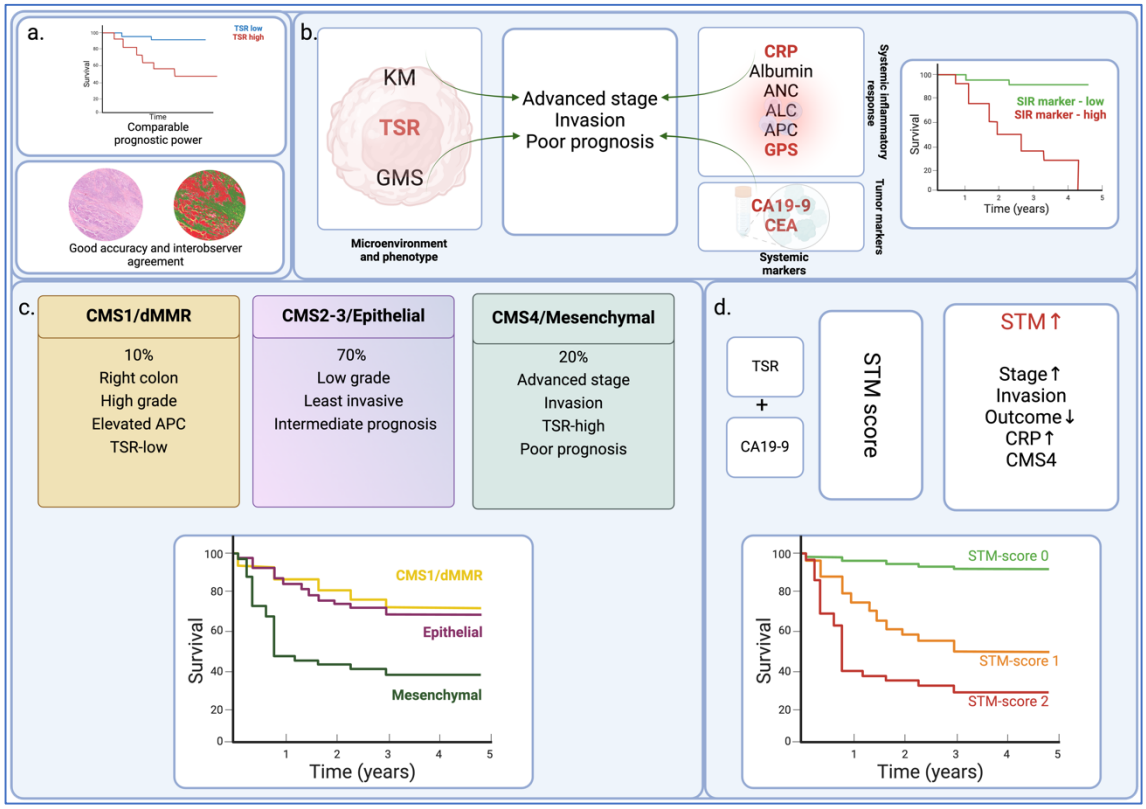

Figure 8.: a. Software assisted TSR evaluation yielded similar prognostic power as TSRvisual with acceptable interobserver agreement and accuracy. b. Both markers of the tissue microenvironment and systemic inflammation were associated with advanced stages, presence of invasion (lymphatic, vascular or perineural) and poor prognosis. c.: The consensus molecular subtypes were associated with biological behaviour, CMS4 represented the most agressive phenotype with poor outcome and TSR-high. Elevated APC was observed in dMMR tumors, otherwise, CMS seemed to be independent of SIR or tumor markers. d. A combined score comprising of TSR and CA19-9 was created, the STM-score. This was associated with poor outcome and adverse clinicopathological features, as well as elevated CRP. List of abbreviations: TSR – Tumor Stroma Ratio, KM – Klintrup-Makinen score, GMS – Glasgow Microenvironment Score, CRP – C-reactive protein, ANC – Absolute Neutrophil Count, ALC – Absolute

Lymphocye Count, APC – Absolute Platelet Count, GPS – Glasgow Prognostic Score, SIR – Sytemic Inflammatory Response, CMS – Consensus Molecular Subtypes, dMMR – Mismatch Repair deficient, STM – Stroma- Tumor Marker score, CA19-9 – Carboanhydrate Antigen 19-9, CEA – Carcinoembryonic Antigen

8. References

1. Costas-Chavarri A, Nandakumar G, Temin S, Lopes G, Cervantes A, Cruz Correa M, et al. Treatment of Patients With Early-Stage Colorectal Cancer: ASCO Resource-Stratified Guideline. J Glob Oncol. 2019;5:1-19.

2. Amin MB, Greene FL, Edge SB, Compton CC, Gershenwald JE, Brookland RK, et al. The Eighth Edition AJCC Cancer Staging Manual: Continuing to build a bridge from a population-based to a more "personalized" approach to cancer staging. CA Cancer J Clin. 2017;67(2):93-9.

3. Lugli A, Zlobec I, Berger MD, Kirsch R, Nagtegaal ID. Tumour budding in solid cancers. Nature Reviews Clinical Oncology. 2021;18(2):101-15.

4. Guinney J, Dienstmann R, Wang X, de Reyniès A, Schlicker A, Soneson C, et al. The consensus molecular subtypes of colorectal cancer. Nature Medicine. 2015;21(11):1350-6.

5. Di Nicolantonio F, Vitiello PP, Marsoni S, Siena S, Tabernero J, Trusolino L, et al. Precision oncology in metastatic colorectal cancer — from biology to medicine. Nature Reviews Clinical Oncology. 2021;18(8):506-25.

6. Kobayashi H, Enomoto A, Woods SL, Burt AD, Takahashi M, Worthley DL. Cancer-associated fibroblasts in gastrointestinal cancer. Nature Reviews Gastroenterology & Hepatology. 2019;16(5):282-95.

7. Schürch CM, Bhate SS, Barlow GL, Phillips DJ, Noti L, Zlobec I, et al. Coordinated Cellular Neighborhoods Orchestrate Antitumoral Immunity at the Colorectal Cancer Invasive Front. Cell. 2020;182(5):1341-59.e19.

8. Wilkinson K, Ng W, Roberts TL, Becker TM, Lim SH-S, Chua W, et al. Tumour immune microenvironment biomarkers predicting cytotoxic chemotherapy efficacy in colorectal cancer. Journal of Clinical Pathology. 2021;74(10):625-34.

9. Klintrup K, Mäkinen JM, Kauppila S, Väre PO, Melkko J, Tuominen H, et al. Inflammation and prognosis in colorectal cancer. Eur J Cancer. 2005;41(17):2645-54.

10. van Pelt GW, Kjær-Frifeldt S, van Krieken J, Al Dieri R, Morreau H, Tollenaar R, et al. Scoring the tumor-stroma ratio in colon cancer: procedure and recommendations. Virchows Arch. 2018;473(4):405-12.

11. Mesker WE, Junggeburt JM, Szuhai K, de Heer P, Morreau H, Tanke HJ, et al. The carcinoma-stromal ratio of colon carcinoma is an independent factor for survival compared to lymph node status and tumor stage. Cell Oncol. 2007;29(5):387-98.
12. Huijbers A, Tollenaar RA, v Pelt GW, Zeestraten EC, Dutton S, McConkey CC, et al. The proportion of tumor-stroma as a strong prognosticator for stage II and III colon cancer patients: validation in the VICTOR trial. Ann Oncol. 2013;24(1):179-85.
13. Hansen TF, Kjær-Frifeldt S, Lindebjerg J, Rafaelsen SR, Jensen LH, Jakobsen A, et al. Tumor-stroma ratio predicts recurrence in patients with colon cancer treated with neoadjuvant chemotherapy. Acta Oncol. 2018;57(4):528-33.
14. Park JH, McMillan DC, Edwards J, Horgan PG, Roxburgh CS. Comparison of the prognostic value of measures of the tumor inflammatory cell infiltrate and tumor-associated stroma in patients with primary operable colorectal cancer. Oncoimmunology. 2016;5(3):e1098801.
15. Alexander PG, Roseweir AK, Pennel KAF, Van Wyk HC, Powell AGMT, McMillan DC, et al. The Glasgow Microenvironment Score associates with prognosis and adjuvant chemotherapy response in colorectal cancer. British Journal of Cancer. 2021;124(4):786-96.
16. Becht E, De Reyniès A, Giraldo NA, Pilati C, Buttard B, Lacroix L, et al. Immune and Stromal Classification of Colorectal Cancer Is Associated with Molecular Subtypes and Relevant for Precision Immunotherapy. Clinical Cancer Research. 2016;22(16):4057-66.
17. Dienstmann R, Vermeulen L, Guinney J, Kopetz S, Tejpar S, Tabernero J. Consensus molecular subtypes and the evolution of precision medicine in colorectal cancer. Nature Reviews Cancer. 2017;17(2):79-92.
18. Roepman P, Schlicker A, Tabernero J, Majewski I, Tian S, Moreno V, et al. Colorectal cancer intrinsic subtypes predict chemotherapy benefit, deficient mismatch repair and epithelial-to-mesenchymal transition. International Journal of Cancer. 2014;134(3):552-62.
19. De Sousa E Melo F, Wang X, Jansen M, Fessler E, Trinh A, De Rooij LPMH, et al. Poor-prognosis colon cancer is defined by a molecularly distinct subtype and develops from serrated precursor lesions. Nature Medicine. 2013;19(5):614-8.

20. Golder AM, McMillan DC, Park JH, Mansouri D, Horgan PG, Roxburgh CS. The prognostic value of combined measures of the systemic inflammatory response in patients with colon cancer: an analysis of 1700 patients. British Journal of Cancer. 2021;124(11):1828-35.

21. Park JH, Fuglestad AJ, Køstner AH, Oliwa A, Graham J, Horgan PG, et al. Systemic Inflammation and Outcome in 2295 Patients with Stage I–III Colorectal Cancer from Scotland and Norway: First Results from the ScotScan Colorectal Cancer Group. Annals of Surgical Oncology. 2020;27(8):2784-94.

22. Climent M, Ryan ÉJ, Stakelum Á, Khaw YL, Creavin B, Lloyd A, et al. Systemic inflammatory response predicts oncological outcomes in patients undergoing elective surgery for mismatch repair-deficient colorectal cancer. International Journal of Colorectal Disease. 2019;34(6):1069-78.

23. Park JH, Watt DG, Roxburgh CSD, Horgan PG, McMillan DC. Colorectal Cancer, Systemic Inflammation, and Outcome. Annals of Surgery. 2016;263(2):326-36.

24. Yamamoto T, Kawada K, Obama K. Inflammation-Related Biomarkers for the Prediction of Prognosis in Colorectal Cancer Patients. International Journal of Molecular Sciences. 2021;22(15):8002.

25. Yakabe T, Nakafusa Y, Sumi K, Miyoshi A, Kitajima Y, Sato S, et al. Clinical Significance of CEA and CA19-9 in Postoperative Follow-up of Colorectal Cancer. Annals of Surgical Oncology. 2010;17(9):2349-56.

26. Liu J-M, Wang Y-Y, Liu W, Xu D, Wang K, Xing B-C. Preoperative CA19-9: a competitive predictor of recurrence in patients with colorectal cancer liver metastases after hepatectomy. International Journal of Colorectal Disease. 2021;36(4):767-78.

27. Yang SH, Jiang JK, Chang SC, Juang CJ, Lin JK. Clinical significance of CA19-9 in the follow-up of colorectal cancer patients with elevated preoperative serum CA19-9. Hepatogastroenterology. 2013;60(125):1021-7.

28. Zhang SY, Lin M, Zhang HB. Diagnostic value of carcinoembryonic antigen and carcinoma antigen 19-9 for colorectal carcinoma. Int J Clin Exp Pathol. 2015;8(8):9404-9.

29. Baqar AR, Wilkins S, Staples M, Angus Lee CH, Oliva K, McMurrick P. The role of preoperative CEA in the management of colorectal cancer: A cohort study from two cancer centres. International Journal of Surgery. 2019;64:10-5.

30. Jia J, Zhang P, Gou M, Yang F, Qian N, Dai G. The Role of Serum CEA and CA19-9 in Efficacy Evaluations and Progression-Free Survival Predictions for Patients Treated with Cetuximab Combined with FOLFOX4 or FOLFIRI as a First-Line Treatment for Advanced Colorectal Cancer. Dis Markers. 2019;2019:6812045-.
31. Kather JN, Weis C-A, Bianconi F, Melchers SM, Schad LR, Gaiser T, et al. Multi-class texture analysis in colorectal cancer histology. Scientific Reports. 2016;6(1):27988.
32. Kather JN, Krisam J, Charoentong P, Luedde T, Herpel E, Weis CA, et al. Predicting survival from colorectal cancer histology slides using deep learning: A retrospective multicenter study. PLoS Med. 2019;16(1):e1002730.
33. Geessink OGF, Baidoshvili A, Klaase JM, Ehteshami Bejnordi B, Litjens GJS, van Pelt GW, et al. Computer aided quantification of intratumoral stroma yields an independent prognosticator in rectal cancer. Cellular Oncology. 2019;42(3):331-41.
34. Millar EK, Browne LH, Beretov J, Lee K, Lynch J, Swarbrick A, et al. Tumour Stroma Ratio Assessment Using Digital Image Analysis Predicts Survival in Triple Negative and Luminal Breast Cancer. Cancers (Basel). 2020;12(12).
35. Kather JN, Pearson AT, Halama N, Jäger D, Krause J, Loosen SH, et al. Deep learning can predict microsatellite instability directly from histology in gastrointestinal cancer. Nat Med. 2019;25(7):1054-6.
36. Sirinukunwattana K, Domingo E, Richman SD, Redmond KL, Blake A, Verrill C, et al. Image-based consensus molecular subtype (imCMS) classification of colorectal cancer using deep learning. Gut. 2021;70(3):544-54.
37. Li T, Yu Z, Yang Y, Fu Z, Chen Z, Li Q, et al. Rapid multi-dynamic algorithm for gray image analysis of the stroma percentage on colorectal cancer. Journal of Cancer. 2021;12(15):4561-73.
38. Zhao K, Li Z, Yao S, Wang Y, Wu X, Xu Z, et al. Artificial intelligence quantified tumour-stroma ratio is an independent predictor for overall survival in resectable colorectal cancer. EBioMedicine. 2020;61:103054.
39. Danielsen HE, Hveem TS, Domingo E, Pradhan M, Kleppe A, Syvertsen RA, et al. Prognostic markers for colorectal cancer: estimating ploidy and stroma. Annals of oncology : official journal of the European Society for Medical Oncology. 2018;29(3):616-23.

40. Nowak JA, Hornick JL. Molecular Evaluation of Colorectal Adenocarcinoma: Current Practice and Emerging Concepts. Surg Pathol Clin. 2016;9(3):427-39.
41. Ten Hoorn S, Trinh A, de Jong J, Koens L, Vermeulen L. Classification of Colorectal Cancer in Molecular Subtypes by Immunohistochemistry. Methods Mol Biol. 2018;1765:179-91.
42. Trinh A, Trumpi K, De Sousa EMF, Wang X, de Jong JH, Fessler E, et al. Practical and Robust Identification of Molecular Subtypes in Colorectal Cancer by Immunohistochemistry. Clin Cancer Res. 2017;23(2):387-98.
43. Mesker WE, Liefers GJ, Junggeburt JM, van Pelt GW, Alberici P, Kuppen PJ, et al. Presence of a high amount of stroma and downregulation of SMAD4 predict for worse survival for stage I-II colon cancer patients. Cell Oncol. 2009;31(3):169-78.
44. Eriksen AC, Andersen JB, Lindebjerg J, dePont Christensen R, Hansen TF, Kjær-Frifeldt S, et al. Does heterogeneity matter in the estimation of tumour budding and tumour stroma ratio in colon cancer? Diagnostic Pathology. 2018;13(1):20.
45. Park JH, Richards CH, McMillan DC, Horgan PG, Roxburgh CSD. The relationship between tumour stroma percentage, the tumour microenvironment and survival in patients with primary operable colorectal cancer. Ann Oncol. 2014;25(3):644-51.
46. Park JH, Powell AG, Roxburgh CS, Horgan PG, McMillan DC, Edwards J. Mismatch repair status in patients with primary operable colorectal cancer: associations with the local and systemic tumour environment. Br J Cancer. 2016;114(5):562-70.
47. Park JH, McMillan DC, Powell AG, Richards CH, Horgan PG, Edwards J, et al. Evaluation of a Tumor Microenvironment–Based Prognostic Score in Primary Operable Colorectal Cancer. Clinical Cancer Research. 2015;21(4):882-8.
48. Park JH, Ishizuka M, McSorley ST, Kubota K, Roxburgh CSD, Nagata H, et al. Staging the tumor and staging the host: A two centre, two country comparison of systemic inflammatory responses of patients undergoing resection of primary operable colorectal cancer. The American Journal of Surgery. 2018;216(3):458-64.
49. Black S, Kushner I, Samols D. C-reactive Protein. J Biol Chem. 2004;279(47):48487-90.

50. Butkiewicz AM, Kemona H, Dymicka-Piekarska V, Matowicka-Karna J, Radziwon P, Lipska A. Platelet count, mean platelet volume and thrombocytopoietic indices in healthy women and men. Thrombosis Research. 2006;118(2):199-204.
51. Long Y, Wang T, Gao Q, Zhou C. Prognostic significance of pretreatment elevated platelet count in patients with colorectal cancer: a meta-analysis. Oncotarget. 2016;7(49):81849-61.
52. Wensink GE, Elferink MAG, May AM, Mol L, Hamers PAH, Bakker SD, et al. Survival of patients with deficient mismatch repair metastatic colorectal cancer in the pre-immunotherapy era. Br J Cancer. 2021;124(2):399-406.
53. Wu T, Mo Y, Wu C. Prognostic values of CEA, CA19-9, and CA72-4 in patients with stages I-III colorectal cancer. Int J Clin Exp Pathol. 2020;13(7):1608-14.
54. Rao H, Wu H, Huang Q, Yu Z, Zhong Z. Clinical Value of Serum CEA, CA24-2 and CA19-9 in Patients with Colorectal Cancer. Clin Lab. 2021;67(4).
55. Lam M, Roszik J, Kanikarla-Marie P, Davis JS, Morris J, Kopetz S, et al. The potential role of platelets in the consensus molecular subtypes of colorectal cancer. Cancer and Metastasis Reviews. 2017;36(2):273-88.
56. Soldevilla B, Carretero-Puche C, Gomez-Lopez G, Al-Shahrour F, Riesco MC, Gil-Calderon B, et al. The correlation between immune subtypes and consensus molecular subtypes in colorectal cancer identifies novel tumour microenvironment profiles, with prognostic and therapeutic implications. European Journal of Cancer. 2019;123:118-29.
57. Fontana E, Eason K, Cervantes A, Salazar R, Sadanandam A. Context matters-consensus molecular subtypes of colorectal cancer as biomarkers for clinical trials. Ann Oncol. 2019;30(4):520-7.
58. Dunne PD, McArt DG, Bradley CA, O'Reilly PG, Barrett HL, Cummins R, et al. Challenging the Cancer Molecular Stratification Dogma: Intratumoral Heterogeneity Undermines Consensus Molecular Subtypes and Potential Diagnostic Value in Colorectal Cancer. Clinical Cancer Research. 2016;22(16):4095-104.
59. Kagawa H, Hatakeyama K, Shiomi A, Hino H, Manabe S, Yamaoka Y, et al. Consensus molecular subtyping improves the clinical usefulness of canonical tumor markers for colorectal cancer. Biomed Res. 2022;43(6):201-9.

9. Bibliography of the candidate's publications (related and not related to the thesis)

9.1.Publications related to the thesis

Jakab, Anna; Patai, Árpád V ; Micsik, Tamás

Digital image analysis provides robust tissue microenvironment-based prognosticators in stage I-IV colorectal cancer patients

HUMAN PATHOLOGY 128 pp. 141-151. , 11 p. (2022)

IF: 3,3

Jakab, Anna; Patai, Árpád V. ; Darvas, Mónika ; Tormássi-Bély, Karolina ; Micsik, Tamás

Microenvironment, systemic inflammatory response and tumor markers considering consensus molecular subtypes of colorectal cancer

PATHOLOGY AND ONCOLOGY RESEARCH 30 Paper: 1611574, 20 p. (2024)

IF: 2,8

9.2.Publications not related to the thesis

Jakab, Anna ; Patai, Árpád ; Micsik, Tamás

Colorectalis carcinoma: molekuláris biomarkerek, precíziós terápia és új perspektívák

ORVOSKÉPZÉS 96 : 3 pp. 387-402. , 16 p. (2021)

IF: -

Micsik, Tamás ; **Jakab, Anna**

A tápcsatorna daganatainak molekuláris genetikája

MAGYAR BELORVOSI ARCHIVUM 75 : 2-3 pp. 72-92. , 21 p. (2022)

IF: -

Micsik, Tamás ; **Jakab, Anna** ; Lehoczki, Csaba ; Patai, Árpád V.

Traditional Serrated Adenoma of the Gallbladder, a Case Report

PATHOLOGY AND ONCOLOGY RESEARCH 28 : 4 Paper: 1610133 , 5 p. (2022)

IF: 2,8

Jakab, A ; Micsik, T

Molekuláris biológia/genetika az emésztőrendszer daganataiban

In: Tulassay, Zsolt (szerk.) Gasztroenterológia

Budapest, Magyarország : Medicina Könyvkiadó (2023) 1,180 p. pp. 1081-1107. , 27 p.

IF: -

10. Acknowledgements

I would like to express my profound gratitude towards all who contributed to this work, namely:
Professor András Matolcsy, MD, DSc and Professor Anna Sebestyén, Dsc for providing excellent infrastructure and work environment.
Viktor Jónás, for his comprehensive introduction to machine learning
Zsófia Zsibai, for precise scanning of HE-slides
Ildikó Krencz, MD, Ph.D., for teaching TMA technique
Members of the Tumor biology and tumor metabolism research group (Gábor Petővári, Ph.D., Dániel Sztankovics, Dorottya Moldvai, PharmD), for teaching and supervising IHC while also providing great company
Anna Tamási and Mónika Paulusz, for their help at the routine IHC laboratory
Éva Mátrai, for her meticulous sectioning of the TMA blocks
Gertrud Forika, MD, Ph.D., for being a great friend and colleague
Professor Péter Nagy, MD, Ph.D., for reviewing the manuscript and taking on the role of opponent for the home viva of this thesis
Márton Cseszla, for being the best husband.
All members of my family, for being my safe place
And least, but not last
Tamás Micsik, MD, Ph.D. and Árpád V Patai, MD, Ph.D. for their constant support and professional guidance